FAR INFRARED OBSERVATIONS OF THE GALACTIC CENTER

Thesis by

Ian Gatley

In Partial Fulfillment of the Requirements

for the Degree of

Doctor of Philosophy

California Institute of Technology

Pasadena, California

1978

(Submitted 1977 August 12)

ACKNOWLEDGEMENTS

It is a pleasure to thank my friends and advisors G. Neugebauer, E. E. Becklin, and M. W. Werner for their guidance and encouragement throughout all phases of this work. They helped overcome some extremely difficult moments.

I also thank the University of Chicago Infrared Group, especially D. A. Harper, R. F. Loewenstein, C. M. Telesco, and H. A. Thronson for their efforts in the development of the experiment. The observations would not have been possible without the heroic efforts of R. Cameron, C. Gillespie, Jr. and the entire staff of the NASA Kuiper Observatory, to whom I am indebted. The Caltech Infrared Group has also been extremely supportive; special thanks are due to G. Forrester. L. Cheung and J. Smith made some of the detectors.

Discussion with many people has helped my understanding of the experimental results. I especially thank S. Beckwith, F. Israel, E. Persson, S. Slutz, S. Willner, and C. G. Wynn-Williams.

I received financial support from Graduate Research Assistantships, from an Earl C. Anthony Fellowship, and from a Robert A. Millikan Fellowship. Support for my research was provided by National Aeronautics and Space Administration grant NGR 05-002-281 which supports far infrared astronomy at Caltech.

I would never have started this work without the constant encouragement of my parents, nor finished it without the love and patience of my wife Cathy. I also owe deepest thanks to her parents, Arnold and Carol Cohen.

ABSTRACT

Maps of a region 10' in diameter around the galactic center made simultaneously in three wavelength bands at 30 μm, 50 μm, and 100 μm with ~ 1' resolution are presented, and the distribution of far infrared luminosity and color temperature across this region is derived. The position of highest far infrared surface brightness coincides with the peak of the late-type stellar distribution and with the H II region Sgr A West. The high spatial and temperature resolution of the data is used to identify features of the far infrared maps with known sources of near infrared, radio continuum, and molecular emission. The emission mechanism and energy sources for the far infrared radiation are analyzed qualitatively, and it is concluded that all of the observed far infrared radiation from the galactic center region can be attributed to thermal emission from dust heated both by the late-type stars and by the ultraviolet sources which ionize the H II regions. A self-consistent model for the far infrared emission from the galactic center region is presented. It is found that the visual extinction across the central 10 pc of the Galaxy is only about 3 magnitudes, and that the dust density is fairly uniform in this region. An upper limit of 10^7 $L_\odot$ is set on the luminosity of any presently unidentified source of 0.1 to 1 μm radiation at the galactic center.

Additional maps in the vicinity of the source Sgr B2 and observations of Sgr C bring the total number of H II regions within 1° of the galactic center studied by the present experiment to nine. The far infrared luminosity, color temperature and optical depth of these regions

and the ratio of infrared flux to radio continuum flux lie in the range characteristic of spiral arm H II regions. The far infrared results are therefore consistent with the idea that the galactic center H II regions are ionized by luminous, early type stars. Steep, systematic gradients in far infrared color temperature and optical depth are seen along the galactic plane between Sgr B2 and G0.5-0.0; the appearance of this area is similar to that of regions of star formation in the spiral arms.

TABLE OF CONTENTS

CHAPTER 2 (Continued)

INTRODUCTION

This thesis consists of two separate but closely related papers which present and discuss observations of the far infrared ($\sim$ 100 μm) emission from the vicinity of the galactic center.

The study of the center of our Galaxy has historically been badly hampered by the fact that the galactic nucleus is not seen at visible wavelengths because of the presence of substantial amounts of interstellar dust in the line of sight. However the extinction by dust decreases with increasing wavelength, and so infrared observations of the galactic center are feasible; studies at near infrared wavelengths ($\sim$ 2 μm) have revealed the nature and spatial distribution of stars in the galactic nucleus.

The role of far infrared astronomy in heavily dust obscured regions is, however, rather different. Naturally the very substantial decrease in dust extinction at these very long wavelengths makes far infrared radiation an excellent probe, but the source of such radiation is in general also dust. This state of affairs comes about in a natural way; the dust simply absorbs radiation at optical wavelengths, becoming warm, and so emits thermally, typically in the far infrared. Therefore, in regions where the local dust absorption optical depth at visual wavelengths is somewhat greater than unity, essentially all the luminosity may be emitted in the far infrared. This is the case for the galactic center.

Far infrared observations of the galactic center will therefore give important information about the total energetics, but that by no

means exhausts their potential. Multicolor observations will give the temperature of the radiating dust, which depends on the location of the dust with respect to the source that heats it, and (because the emission is almost always optically thin) the optical depth gives the column density of radiating dust.

Until recently it has not been feasible to exploit these advantages of far infrared astronomy for a simple reason: the earth's atmosphere is opaque in the far infrared. This opacity is chiefly caused by water vapor, and so it is possible to overcome the problem by operating from airborne platforms typically at altitudes greater than 40,000 ft. Observations have been carried out from rockets, balloons and aircraft, but in almost every case the payload restrictions have required that the telescope be small, which has limited the angular resolution of such observations to many arcminutes. The exception is provided by the NASA Gerard P. Kuiper Airborne Infrared Observatory, a 91-cm telescope mounted in a C-141 aircraft. From this facility it is possible to make observations at wavelengths around 100 μm with angular resolution of about one arcminute or less. All the far infrared observations described in this thesis were made from this aircraft.

The instrument used for the present observations is a three-color far infrared photometer, which measures the radiation from the same ~ 1' field of view simultaneously at wavelengths of 30 μm, 50 μm, and 100 μm. A single measurement with this instrument therefore determines both luminosity and temperature. The overwhelming advantage of such a simultaneous measurement over sequential measurements is most clearly seen in a region

of extended emission in which temperature gradients are present. With the present instrument, study of such a region poses no problem, but in the case of comparison of nonsimultaneous measurements at different wavelengths, it is generally very difficult to distinguish between temperature gradients and relative pointing errors. Since the whole of the galactic plane within $\sim 1°$ of the galactic nucleus is a source of bright far infrared emission, the three-color photometer is the ideal instrument for its study. The maps presented in this thesis represent an improvement in spatial resolution of a factor of five over previous work in the far infrared, and constitute the first far infrared temperature study of the region. The temperature information is crucial in the understanding of such a complex region.

In the first paper (Chapter 1) maps of a 10' diameter region around the galactic nucleus are presented and the features of the maps are identified by comparison with near infrared, radio and molecular data. Quantitative analysis is confined in Chapter 1 to a study of the very extended emission from the galactic plane, which is shown to be thermal radiation from dust heated primarily by the late-type stellar population.

In the second paper (Chapter 2) attention focuses on the discrete far infrared sources present in the maps. These turn out to be H II regions. Additional measurements of the galactic center H II regions Sag B2, G0.5-0.0, and Sgr C are presented. Comparison of this sample of H II regions with well studied spiral arm H II regions shows that the galactic center is a region of recent star formation.

CHAPTER 1

THE GALACTIC CENTER

I. INTRODUCTION

Physical conditions at the center of a galaxy are unique. The high space density of both mass and luminosity allows the possibility of phenomena which do not occur elsewhere, making galactic nuclei prime observational targets and regions of theoretical interest. Therefore, it is important to examine the center of our own galaxy since its relative proximity allows details to be distinguished on a finer scale than in external galaxies.

Intense far infrared* radiation, with a luminosity on the order of 10^8 $L_\odot$, has been detected from an extended region (0.5°) around the galactic center (Hoffmann and Frederick 1969; Hoffmann, Frederick and Emery 1971). This radiation has generally been interpreted as thermal emission from dust, although nonthermal contributions have also been discussed (e.g., Burbidge and Stein 1970). Since almost all of the energy observed from the galactic center is at far infrared wavelengths, it is important to make observations with the highest possible spatial and spectral resolution in this wavelength range. Prior to 1975, the highest spatial resolution achieved in far infrared measurements of the galactic center was 3!5 (Low and Aumann 1970).

*The term "far-infrared" is used for wavelengths $25\ \mu < \lambda < 130\ \mu$ in this paper.

This paper reports mapping with a resolution of $\sim$ 1' ($\sim$ 3 pc at an assumed distance of 10 kpc for the galactic center) of a region around the galactic center about 10' in diameter at wavelengths of 30 μ, 50 μ, and 100 μ. An important feature of the present experiment is that measurements of the flux from a single field of view on the sky are made simultaneously at the three wavelengths. In this way the experiment measures both surface brightness and color temperature directly.

The far infrared observations presented in this paper were part of a series of experiments conducted from NASA's Gerard P. Kuiper Airborne Infrared Observatory to study the galactic center. The present work is complementary to the other experiments of this series (Harvey, Campbell and Hoffmann 1976; Telesco and Harper 1975) which mapped the central few minutes of the Galaxy in the far infrared with high resolution (20"), and also to the 1' resolution far infrared balloon-borne survey of Fazio (1976). In addition to the far infrared maps, we also present in this paper a measurement of the 1 millimeter continuum radiation from the central 1' of the Galaxy, and a new representation of the 2.2 μ map of Becklin, Neugebauer, and Early (1974).

The structure of this paper is as follows. We review relevant previous observations of the galactic center region at radio and infrared wavelengths in § II and discuss the details of instrumentation, observations, and data reduction in § III. A comparison of the far infrared surface brightness and color temperature maps with near infrared, radio continuum, and molecular maps then leads to identification of the various features of the far infrared emission (§ IV). In § V it is argued that

the far infrared emission is thermal radiation from dust heated by known sources of optical and ultraviolet radiation and in § VI a model calculation confirms the plausibility of this hypothesis. The main results of this study are reviewed and summarized in § VII.

II. PREVIOUS OBSERVATIONS OF THE GALACTIC CENTER AND THEIR INTERPRETATION

In this paper we shall frequently allude to observations of the galactic center at wavelengths other than the far infrared. In view of the variety of these observations we present here a summary of those which are most relevant to the interpretation of the new far infrared data.

a) Near Infrared

The first infrared observations of the center of the Galaxy were made by Becklin and Neugebauer (1968) [hereafter designated BN] who discovered an extended 2.2 μ source centered at the radio source Sagittarius A. The position of peak 2.2 μ surface brightness is conventionally taken to be the position of the center of the Galaxy. The similarity of the near infrared properties of the galactic center source to those of the center of M31 led BN to interpret the 1-3 μ radiation as stellar radiation from a distribution of predominantly late type stars. Under this hypothesis the stellar density within the central 1 pc of the Galaxy is 10^7 times that in the solar neighborhood. BN also concluded that the visual extinction to the galactic center is about 27 magnitudes. Recently individual near infrared sources within the central 0.5 of the

Galaxy have been resolved (Becklin and Neugebauer 1975) and in some cases identified as late type giants and supergiants (Neugebauer et al. 1976). The similarity of the near infrared color of these individual stars to that of the integrated radiation from the source for fields of view up to 110" both strengthens the interpretation of the extended near infrared emission as starlight and suggests that most of the 27 magnitudes of visual extinction to the source are distributed along the line of sight rather than local to the galactic center (Becklin et al. 1977).

Sanders and Lowinger (1972) drew on BN's conclusions to derive a simple model for the space density of stellar luminosity, L(S), on the assumption that most of the power arises from late-type stars with a mean surface temperature of 4000 K;

$$L(S) = \frac{2.5 \times 10^5}{S^{1.8}} \quad L_\odot \text{ pc}^{-3} \qquad (1)$$

where S (pc) is a radial coordinate on the major axis of an ellipsoidal coordinate system whose axis of azimuthal symmetry passes through the galactic center and is perpendicular to the galactic plane.

b) Radio Continuum

The present observational status of Sgr A at radio continuum wavelengths is described by Ekers et al. (1975) and Pauls et al. (1976). They showed that the source is resolved into two major components

designated Sgr A East and Sgr A West, which are separated by about 2'; Sgr A East is thought to be a supernova remnant. Sgr A West is an H II region coincident with the peak of the stellar distribution seen at 2.2 μ. Additional radio structure including isolated H II regions and a background of both thermal and nonthermal radiation is seen within a few arcminutes of Sgr A. At 10.7 GHz the thermal and nonthermal contributions to the radio emission from the central 6' of Sgr A are roughly comparable (Pauls et al. 1976).

The amount of thermal radio continuum emission observed from an H II region such as Sgr A West can be used directly to estimate a lower limit to the luminosity of the sources which ionize the H II region. This lower limit, E_M, is equal to the rate of recombination in the ionized region multiplied by the ionization energy of hydrogen. The quantity E_M is easily derived from the observed thermal radio continuum emission because both are proportional to the volume of the region and the square of the electron density (Osterbrock 1974). The total luminosity of the ionizing source is greater than E_M by a factor f, which depends on the detailed properties of the source and typically lies between 3 and 30. For Sgr A the value of E_M is $\simeq 10^6\ L_0$; this is then a lower limit to the luminosity of the ionizing sources. If it is assumed that the ionization is produced by O stars, $f \approx 3$ (Panagia 1973), and the total luminosity provided by such O stars within the central 1' of the Galaxy is $\sim 3 \times 10^6\ L_0$. This is somewhat greater than the luminosity inferred above from the near infrared data for the late-type stars within the

same volume; however, the O stars would not contribute significantly to the near infrared radiation from the region (Neugebauer et al. 1976).

c) Molecular

Although molecular emission is seen from the galactic center region, there is no molecular concentration precisely coincident with the position of Sgr A West and the highest stellar density. For example, both the CO emission (Solomon et al. 1972; Liszt, Sanders, and Burton 1975) and the OH absorption (Bieging 1976) in this region are most intense about 3 arcminutes to the east of Sgr A. The position of these molecular clouds along the line of sight is not known, and they may lie somewhat in front of or behind the galactic center (Scoville 1972).

III. INSTRUMENTATION AND OBSERVATIONS

a) Airborne Observations

The far infrared observations described here were made at an altitude of 12.3 km from the Gerard P. Kuiper Airborne Infrared Observatory, a 91 cm gyrostabilized telescope mounted in a C-141 aircraft (Cameron, Bader, and Mobley 1971) flying out of Hawaii during 1975 August. The detectors are bolometers operated at 2°K contained in a helium-cooled dewar mounted at the bent Cassegrain focus of the telescope. Direct viewing of the focal plane of the telescope with a television system through a warm dichroic mirror allows guiding on field stars. Inside the dewar (Fig. 1), cold restrahlen reflection beamsplitters allow simultaneous observation of the same

field of view in three well-defined bands at 30 μ ($\Delta\lambda \simeq 10$ μ), 50 μ ($\Delta\lambda \simeq 25$ μ), and 100 μ ($\Delta\lambda \simeq 45$ μ). The measured spectral response of each of these bands is shown in Figure 2. The simultaneous observation of the same field of view at three different wavelengths facilitates reliable estimates of the variation of color temperature across a source; it is this feature which distinguishes this from most other far infrared mapping experiments. This simultaneity is especially useful in the case of observing from the airborne telescope, because the alt-azimuth mounting produces a continuously variable rotation of the field of view in the focal plane. Since guiding of the telescope is performed using offset field stars, the field rotation makes it difficult to ensure that precisely the same point on the sky is observed if measurements at different wavelengths are made sequentially; a related problem is that the location of the chopped reference beam on the sky is different when the same point is measured at different times.

The observations were made using the oscillating secondary mirror with a 4' beam spacing in azimuth. The source was mapped in a "step-and-integrate" mode. A single 10 second integration was taken before advancing 30" in the direction of chopping to the next sample point. A typical scan is 12' long. The signal-to-(rms) noise ratio in one 10 second integration at the position of peak surface brightness on Sgr A is $\sim$ 5:1 at 30 μ, $\sim$ 50:1 at 50 μ, and $\sim$ 30:1 at 100 μ. The position of peak surface brightness was measured between scans as a check on sensitivity and guiding accuracy. The absolute positional accuracy at any point of the maps, determined from repeated measurements of the position of peak surface brightness relative to stars, is $\sim$ 15". Most

of the region studied in the far infrared was mapped on each of two nights; the two sets of data are in good agreement.

The beam profiles were mapped on Saturn, the diameter of which at the time of observation was 17". The beams were approximately Gaussian in shape and the full width at half maximum of the beam was 40" at 30 μ and 50 μ, and 55" at 100 μ. Flux calibration was achieved by observations of Jupiter, for which the far infrared energy distribution was assumed to be given by a model based on measurements from Pioneer 10 (Ingersoll et al. 1976). The diameter of Jupiter at the time of these observations was 43". The measured beam profile has been integrated over the planet disk in order to calculate the flux reaching the detector at each wavelength. The overall (1σ) uncertainty in the resulting flux calibration is estimated to be 20 percent.

b) Ground-based Observations

The 1 millimeter continuum observation of the central 1 arcminute of the Galaxy was made in 1975 October at the prime focus of the Hale 5 m telescope during twilight hours. A conventional chopping infrared photometer was used with a 1' beam and a 4' beam spacing in declination; details of the instrumentation are given by Elias et al. (1977). The 2.2 μ map was constructed from 19 successive right ascension scans made on the 1 m telescope at Las Campanas, Chile (Becklin, Neugebauer and Early 1974). A single measuring beam (FWHM = 1!2) on the sky was used in order to avoid the problems inherent in position switching on extended sources; the zero of the map was chosen 1^{o} west of the galactic center. The new map is consistent with that of BN, but should give a more accurate picture of the extended features of the galactic center at 2.2 μ.

IV. DATA

a) Construction of the Maps

Maps of the galactic center region at wavelengths of 2.2 μ, 30 μ, 50 μ, and 100 μ are shown in Figure 3. The region observed at the three far infrared wavelengths is delineated by the dashed lines crossing the maps diagonally. At 2.2 μ a substantially larger region was mapped than is shown; see the photograph constructed from the same data by Becklin et al. (1974).

For the far infrared mapping the direction of scanning on the sky changes as a function of time because of the field rotation. During the present observations the scan direction was between 92^{o} and 122^{o} east of north, that is, approximately perpendicular to the plane of the Galaxy. The spacing between adjacent scans is approximately 30"; the scans are not precisely parallel to one another because of rotation of the field. The scans have been deconvolved to remove the effects of spatial chopping under the assumption that the flux in the reference beam is zero at both ends of each scan. The maps of Hoffmann, Frederick and Emery (1971) and Alvarez et al. (1974) show this to be a reasonable assumption; from their maps the residual flux at the ends of the scans into our beam can be estimated to be less than 10 percent of that from the position of peak surface brightness. Nevertheless, it is this uncertainty in the determination of the zero level which limits the reliability of the mapping at 50 μ and 100 μ.

Figure 4a is a map of the far infrared luminosity of the galactic center region constructed by integrating the maps of Figure 3, while Figure 4b is a 50 μ to 100 μ color temperature map. (The color temperature is defined as the temperature of a Planck curve fit through the data.) The relative temperature distribution across this map is accurate to ~ 5K, but the calibration uncertainties allow the possibility that all temperatures could be systematically raised or lowered by up to ~ 15K. Figures 4c and 4d are a 10.7 GHz radio continuum map derived from Pauls et al. (1976) and a molecular ^{12}CO emission map derived from Solomon et al. (1972); these maps, which have similar angular resolution, are included for comparison with, and identification of, features of the far infrared maps.

b) The Features of the Maps

At all three far infrared wavelengths the maps consist of a dominant bright source, coincident with the galactic center, plus a variety of fainter sources and regions of extended emission. Comparison of these maps with each other and with radio, molecular line emission, and 2.2 μ maps show an unexpectedly wide range of phenomena. In particular:

(1) The main peak of far infrared emission coincides with the peak of the 2.2 μ emission and with the radio continuum source Sgr A West. It does not coincide with the positions of the strongest CO emission. The far infrared peak is the hottest point on the map and is extended at all three wavelengths. The diameter of the source increases with increasing wavelength; this means that the color temperature of the source decreases away from the center.

(2) The two sources seen on the 30 μ map to the northwest of the peak appear as bright features at all three far infrared wavelengths. These sources have a higher color temperature than do the immediately

surrounding areas and coincide with the known H II regions G0.01+0.02 and G0.07+0.04 (Pauls et al. 1976). A third H II region identified in Figure 4c, G0.01-0.12, also appears as a discrete hot source at far infrared wavelengths.

(3) There is a local maximum in the 50 μ and 100 μ surface brightness about 5 arcmin north of Sgr A. This source coincides with a minimum in the radio map and is also much cooler than the H II regions or the Sgr A source.

(4) The molecular emission peaks coincide with minor peaks in the infrared luminosity distribution; the region of strong molecular emission is the coldest on the map.

(5) There is no obvious far infrared feature corresponding to the nonthermal radio source Sgr A East.

(6) At 50 μ and particularly at 100 μ there is much extended emission, mainly to the north of Sgr A. Both the 2.2 μ emission from stars and the radio emission are also extended in this direction.

c) Profiles and Energy Distribution

Figure 5 shows profiles of the observed emission through the galactic center parallel to and perpendicular to the galactic plane. The far infrared profiles are constructed from the maps (Figure 3) presented in this paper. Since the direction of scanning when taking data was approximately across the plane of the Galaxy, the minor axis profiles are almost the same as the scans through the peak from which the maps were made. The far infrared luminosity profiles are constructed

by integrating the observed far infrared energy distributions from 25 μ to 130 μ. The 2.2 μ profiles are taken from Figure 5 of BN and have the same resolution (0!8) as the present far infrared data.

Figure 5 shows that the source is extended along both major and minor axes at all observed wavelengths. The far infrared profiles are successively broader at longer wavelengths, implying that the color temperature falls in all directions away from the peak. The angular resolution of the present observations is not high enough to resolve the peak into the two components seen by Harvey et al. (1976) and Telesco and Harper (1975).

Figure 6 shows the energy distribution from 30 μ to 1 mm of the central 1' of the Galaxy. This energy distribution was obtained by spatial integration of the surface brightness maps at 30 μ, 50 μ, and 100 μ (Fig. 3) and by direct measurement at 1 mm. The 50 μ to 100 μ color temperature is $\sim$ 100 K whereas the 50 μ brightness temperature is $\sim$ 40 K. The 25 μ to 130 μ luminosity of the central 1' is 2.3 x 10^6 $L_\odot$. The observed 1 mm flux is barely in excess of the free-free emission expected from Sgr A West.

V. DISCUSSION

a) Emission Mechanism

The two most frequently discussed mechanisms which are capable of producing an energy distribution with the shape of that of the galactic center (Fig. 6) are synchrotron emission and thermal emission from dust grains (Burbidge and Stein 1970). In the synchrotron interpretation the steep decline of the spectrum between 100 μ and 1 mm is

attributed to self absorption, but a difficulty arises in that the derived magnetic field for a source 1' in size is unreasonably large unless the existence of a cluster of several hundred compact synchrotron sources is postulated. The present data pose another extremely serious problem for the synchrotron picture, because the size of the source increases with increasing far infrared wavelength.

On the other hand, the present data provide very strong support for the idea that the far infrared radiation is thermal emission from dust. In particular, the wavelength dependence of the source size is a natural result of a temperature gradient in the dust which is produced by heating by a centrally concentrated energy source. Moreover, the observed energy distribution (Figure 6) is similar to that of other far infrared sources where the emission is very probably thermal emission from dust, as, for example, in the Orion Nebula region (Harper 1974; Werner et al. 1976). Therefore we feel that thermal emission from dust is by far the most likely mechanism for the far infrared emission from the galactic center. This interpretation will be adopted for all that follows.

b) Heating of the Dust

One of the most important questions which can be posed about the galactic center is the nature of the source of luminosity which heats the dust which radiates in the far infrared. In the galactic center region there exists a stellar population which is observed in the near

infrared; both the luminosity and the energy distribution of this stellar distribution can be inferred by analogy with the energy distribution of M31 and other galaxies. There also exists a strong thermal radio source, Sgr A West, which must be ionized by an energy source other than the late-type stars. The total luminosity and the energy distribution of this source cannot be determined uniquely; however, the minimum luminosity of this source, E_M, can be inferred from the radio continuum emission as discussed in § II. In addition, there might exist in the galactic center substantial luminosity sources other than those which are inferred from the near infrared and radio continuum observations.

In Figure 7 we plot the power radiated by the stellar distribution and the minimum power supplied by the ionizing sources within circular aperture diameters from 0!5 (1.5 pc) to 30' (90 pc) centered on the position of peak emission. Also shown in the figure is the total power reradiated by the dust at far infrared and submillimeter wavelengths. It is clear that the known luminosity sources can provide sufficient power to heat the dust and produce the observed infrared radiation. This is particularly true if Sgr A is typical of other galactic H II regions where the total luminosity of the ionizing sources is 3 to 6 times E_M (Furniss, Jennings, and Moorwood 1974). Although Figure 7 does not place a limit on unknown sources of luminosity at the galactic center, it does show that they are not needed to account for the observed far infrared radiation. This point is discussed further in § VIg.

It is interesting to speculate on the relative importance of the late-type stars and the ionizing sources in producing the infrared

luminosity from the galactic center. Because both sources of luminosity peak at the same position and can supply comparable amounts of energy, it is not possible to distinguish effects due to one or the other within the central few parsecs. Away from the central few parsecs, both the far infrared radiation and the stellar distribution are elongated along the galactic plane, while the radio flux is more circularly symmetric. This suggests that stellar heating may be more important in the outer regions. In summary, it is clear that if either the late-type stars seen at 2.2 μ or the ionizing sources deduced from radio observations were removed from the galactic center region, the remaining component could produce a far infrared source similar to, but fainter than, the observed source.

Several peripheral discrete H II regions are seen in Figure 4c; these all appear as bright hot spots in the far infrared maps. The luminosity of each of these H II regions is a few x 10^5 L_0, typical of galactic H II regions and consistent with their being ionized by a single early type star (Panagia 1973). They will be considered, along with Sgr B2, in Chapter 2 .

The molecular clouds are seen as discrete luminosity sources and are relatively cold. For many galactic molecular clouds there is evidence of an internal heat source consisting of a cluster of young or forming stars; the color temperature of the far infrared emission from the molecular clouds east of Sgr A, $\sim 40^{\circ}K$, is comparable with that seen from molecular clouds which are heated by such a cluster (Werner, Becklin, and Neugebauer 1977). However, the present data require the existence of such an internal heat source only if the clouds lie some

distance along the line of sight away from the galactic center, since the luminosity of the late-type stellar distribution (BN) at the projected distance of the clouds from the galactic center is comparable to the far infrared luminosity of the clouds. If the clouds are heated by the late-type stars, the steep drop in color temperature in this region can probably be attributed to self-shielding of the grains from the heat source (see also § Ve).

c) Distribution and Density of the Dust

In this section, we present arguments based directly on the data which suggests that the dust density in the galactic center region is both low and uniform. These qualitative arguments are supported by the detailed model presented in § VI. The optical depth of the far infrared emission at 50 μ, $\tau_{50\ \mu}$, can be estimated by a comparison of the 50 to 100 μ color temperature to the 50 μ brightness temperature. Under the assumptions that the grain emissivity is proportional to λ^{-1} (§ VIc) and that all grains along each line of sight have the same temperature, it is found that $\tau_{50\ \mu} \sim 0.05$ at almost every point on the source except for the regions of strongest CO emission. This indicates that the column density of dust is constant over much of the source and suggests that the volume density of dust is fairly uniform throughout the whole of the region mapped, that is, within about 15 pc of the galactic center. In contrast, the space density of stars falls by a factor of more than 100 between 1 and 15 pc (the stellar density, given in § II, falls as radius $^{-1.8}$). The ionized gas density, too, falls from $n_e \sim 10^4$ cm^{-3} in the central 1 pc of Sgr A West (Balick and Sanders 1974) to $n_e \sim 10^2$ cm^{-3} at about 15 pc from the center (Pauls et al. 1976).

Additional evidence indicating that in the galactic center region the dust density is both low and uniform is presented in Figure 5, which compares the 2.2 μ emission profiles along and across the galactic plane with the far infrared luminosity profiles. It has been argued that heating of the dust both by the stellar distribution responsible for this 2.2 μ profile and by the sources which ionize the H II regions is important. Although the spatial distribution of the ionizing sources in the galactic center region is unknown, comparison of Figures 3a and 4c suggests that, within the central few arc minutes of the Galaxy, these sources are distributed in a manner similar to the late type stars. Therefore, we assume that the 2.2 μ profile has very roughly the shape of the distribution of the ultraviolet and optical heating sources. The far infrared profile shows the distribution of reradiated energy. Since this reradiation of energy occurs at wavelengths where the extinction by the dust is extremely small, comparison of the widths of the 2.2 μ and far infrared profiles gives information about the absorption optical depth of the dust to the heating radiation. If this absorption optical depth were high the heating radiation would be converted into the far infrared close to its source, and the shape of the two profiles would be almost identical. However, for the region as a whole, Figure 5 shows that the far infrared luminosity profile is significantly wider than the 2.2 μ profile. This suggests that the dust is optically thin to optical and ultraviolet radiation on the spatial scale of the present observations, that is, a few parsecs. Moreover, the greater width of the far infrared profile supports the hypothesis that the dust is distributed uniformly through the region, for if the dust density increased sharply into the center, the luminosity profile would tend to fall steeply away from the central density enhancement.

The above arguments based on the optical depth and distribution of the far infrared emission suggest that the density of dust is fairly low in the center of the Galaxy, producing one optical depth at visual wavelengths in $\sim$ 10 pc. Additionally, the low flux measured at 1 mm indicates that there is no strong concentration of dust at the galactic center (cf. Westbrook et al. 1976). The low value for the extinction due to dust in the galactic center region inferred from the present data is consistent with the conclusion drawn from near infrared observations (§ II) that most of the 27 mag of visual extinction in front of the galactic center are distributed along the line of sight and not local to the source (Becklin et al. 1977).

d) Molecular Clouds Near the Galactic Center

Figure 4d shows the location of the molecular clouds near the galactic center. The infrared color temperature (Fig. 4b) reaches its lowest value in the whole of the map at the positions of strong molecular emission, which are also conspicuous in the far infrared luminosity map. The optical depth of the 50 μ emission from these regions is $\tau_{50\ \mu} \sim 0.2$; this is four times the value elsewhere. If the line of sight extent of the core of each cloud is similar to its projected size, then this four-fold increase in optical depth indicates that the dust density in the molecular clouds is an order of magnitude greater than elsewhere in the region mapped.

It is important to note that the primary peak in the far infrared emission from the galactic center does not coincide with a molecular emission peak. Lower angular resolution observations (Scoville, Solomon, and

Jefferts 1974) have shown a strong correlation between CO brightness temperature and 100 μ flux, but this correlation is not seen in detail at the higher resolution of the present observations. The properties of the galactic center region, therefore, emphasize the fact that the high densities associated with molecular clouds are by no means necessary for intense far infrared emission. All that is required to produce efficient conversion of luminosity from visible to far infrared wavelengths is a visual absorption optical depth of order unity local to the source.

e) Visibility of Secondary Far Infrared Features

In the previous section it was shown that most of the far infrared radiation from the galactic center region is provided by emission from uniformly distributed dust heated by the extended stellar distribution. The parameters which determine the nature of the observed far infrared radiation (for some particular assumed type of dust grain) are the density of the dust and the luminosity available to heat it; the discrete features seen in the outer regions of the far infrared maps can be attributed to local changes in one or both of these parameters.

The dust distributed uniformly throughout the region provides absorption optical depth unity to the radiation which heats it in about 10 pc (§ Vc). Therefore, if an extra source of luminosity is introduced at some point in this distribution it will produce a local enhancement in the far infrared luminosity, and, because the individual grains get hotter, the color temperature of the emission will increase. Examples

of this phenomenon are the H II regions near the galactic center, which appear as hot, luminous points in the far infrared maps; the extra source of luminosity in each case is probably the ultraviolet source which ionizes the H II region.

Because most of the radiation which heats the dust is absorbed within 10 pc of its point of origin, very little luminosity escapes the region at optical or ultraviolet wavelengths. Since essentially all the available power is converted into the far infrared at this spatial dust density, the effect of increasing the amount of dust cannot be to increase the total far infrared luminosity from the region as a whole. However, modest increases in dust density in compact areas can enhance the local surface brightness by absorbing radiation which would have otherwise crossed without being absorbed. Provided the density enhancement is only slight, and exists only over a distance small compared to the absorption length, the dust grains will be as hot in the high density area as elsewhere. An example may be provided by the "hole" in the radio continuum map near G0.0+0.0 (Fig. 4c). It appears as a luminous area at 50 μ and 100 μ, but its color temperature is the same as at nearby positions.

If the dust density is further enhanced, the power absorbed by each individual grain is reduced due to shielding by the other grains, and the grains are colder. Therefore the color temperature of the far infrared emission is reduced. This could be the situation at the molecular clouds, which appear quite dense and have a low color temperature.

VI. A MODEL FOR THE FAR INFRARED EMISSION FROM THE CENTRAL 5' OF THE GALAXY

a) Rationale

We have argued that the far infrared radiation from the galactic center is optically thin thermal radiation from dust grains, distributed uniformly and heated both by the late-type stars and by the ultraviolet sources which ionize the H II regions. To check the consistency of this interpretation a model based on these assumptions has been constructed. This model is neither unique nor highly precise, but it does have the virtue that it rules out several potential alternatives.

b) Details of the Model

The model consists of a uniform space density of dust heated both by the stellar distribution and by a point source of luminosity approximating the ultraviolet source which ionizes Sgr A West. The aim is to explain the distribution of far infrared surface brightness in the central region away from the subsidiary sources. The data to which the model will be fit are taken along the major axis of the far infrared isophotes to the north of Sgr A.

The spatial density of late-type stellar luminosity is assumed to be that deduced by Sanders and Lowinger (1972) and given in § II. This luminosity is assumed to be radiated at a single wavelength of 0.7 μ (near the peak of a 4000 K blackbody). The ultraviolet source which

powers the H II region Sgr A West is included as a point source of luminosity $L = 3 \times 10^6 L_\odot$ at the galactic center. The choice of this luminosity is arbitrary since the nature of the ionizing source is unknown; the present value is in the range expected if the ionization is by O stars. The grain absorption efficiency is assumed to be three times greater for the radiation from the ultraviolet source than for the 0.7 μ stellar radiation. An extended source of ultraviolet radiation is not explicitly included; presumably, its effects would be similar to those of the extended stellar distribution.

Because of the observed low optical depth of both far infrared emission and near infrared extinction, reabsorption of the infrared radiation from the heated dust is ignored, but attenuation of the heating radiation by the dust is included. We simply seek a value for the absorption of starlight per unit path length by the dust, K, which will account for the observed spatial distribution of far infrared emission; the corresponding value for the dust density is discussed in § VIf. The model calculation has been performed in three dimensions out to a distance of 30 pc from the center and then integrated along the line of sight to be compared with the data. Initially we seek to account only for the observed luminosity profile because this can be done without detailed knowledge of the emission efficiency of the grains in the far infrared. For any reasonable choice of far infrared emission efficiency, about 2/3 of the reradiated luminosity falls in the 25 to 130 μ band. In § VId we shall discuss the prediction of color temperature for different assumed grain efficiencies.

c) Predicted Luminosity Profiles

Figure 8a shows the observed and predicted far infrared surface brightness as a function of distance from the galactic center, as well as the separate contributions predicted from the central ultraviolet point source and the late-type stars. Although the initial model calculations were made for a constant value of K, it was found that a modest increase in K in the central few parsecs improved the fit. The predicted profile shown in Figure 8a is generated for a dust distribution which has $K = 0.07$ mag pc^{-1} at 0.7 μ for distances greater than 3 pc from the center, with an increase in K by a factor of two within 3 pc.

As Figure 8a shows, the luminosity between 5 and 14 pc is supplied solely by the extended stellar distribution in this model. The effect of increasing or decreasing K in this region is shown in Figure 8b. The fit to the data is significantly worse in either case. Also shown in Figure 8b is the predicted profile for a gradient of K with the same radial dependence as that of the stars beyond 5 pc ($\propto$ radius $^{-1.8}$). This case is clearly excluded by the observations.

d) Properties of the Grains

The model can be extended to predict color temperatures given the wavelength dependence of the grain absorption efficiency $Q(\lambda)$. For small grains two tractable possibilities exist at long wavelengths: (1) $Q(\lambda) \propto \lambda^{-1}$ corresponding to the most efficient grains, where the effect of long wavelength impurity oscillators is saturated (Purcell 1969); (2) $Q(\lambda) \propto \lambda^{-2}$ corresponding to grains without long wavelength

resonances (Aannestad 1975). The latter case has been predicted theoretically to apply at sufficiently long wavelengths. The present experiment provides information on Q (λ) out to $\lambda \simeq 150$ μ, the approximate limit of the 100 μ passband.

In Figure 9 we present the predicted color temperature corresponding to the best fit model luminosity profile for two cases: (1) a λ^{-1} dependence from 0.7 μ through the far infrared; (2) a λ^{-1} dependence from 0.7 μ to 30 μ and a λ^{-2} dependence longward of 30 μ. The calculated temperatures are, in fact, not sensitive to the form of Q (λ) at wavelengths $\lambda \gtrsim 150$ μ because, for the range of temperatures emerging from the calculations, little of the energy of an individual grain is radiated at these long wavelengths. The observed 50 μ to 100 μ color temperature is also displayed in Figure 9. From Figure 9 it is seen that Q (λ) $\propto \lambda^{-1}$ in the far infrared provides good agreement between the model and the observations, but that Q (λ) $\propto \lambda^{-2}$ does not; the color temperatures predicted for Q (λ) $\propto \lambda^{-2}$ are appreciably higher than those observed. Thus the data appear to favor a λ^{-1} dependence over a λ^{-2} dependence; however, this conclusion is affected by uncertainties in the calibration and, especially, in the assumptions of the model and may not be unique. The physical grain temperature for the best fit model with Q (λ) $\propto \lambda^{-1}$ varies smoothly from 80°K at 1 pc from the center to 50°K at 10 pc from the center. It is interesting to note with regard to the problem of grain efficiency that observations of the dust-embedded carbon star IRC+10216 have been interpreted as showing Q (λ) $\propto \lambda^{-1}$ for this object in the wavelength range 50 $\mu < \lambda < 1000$ μ (Campbell et al. 1976).

e) Some Consequences of the Model

The model calculation presented above is not unique, but it serves to illustrate the type of input parameters necessary to fit the data.

The items which must be included are: (1) A dust distribution which produces the observed constant optical depth of the far infrared emission. The simplest choice satisfying this condition is that of almost constant dust density, but other dust distributions may be allowable; (2) an extended source of luminosity to produce the observed slow fall-off of surface brightness and color temperature away from the center. The far infrared luminosity profile produced by a central point source is shown in Figure 8a; it falls more steeply than the observed profile. Whatever the nature of this extended heat source, the energy per unit volume supplied by it must be comparable to that formulated for the late-type stars (Eq. 1). An attraction of using this stellar distribution in the present model is that its fall-off accounts naturally for the size of the far infrared source. Furthermore, the ellipticity of the stellar distribution leads to an elliptical far infrared source; in fact, the ellipticity predicted by the model agrees well with that observed. (3) A compact bright central source of luminosity $L \sim 3 \times 10^6$ $L_\odot$ to account for the high far infrared luminosity of the central region of the galactic nucleus must also be included in the model. The ultraviolet source which ionizes Sgr A West may provide this luminosity.

The model also serves explicitly to exclude some scenarios. In particular (1) the spatial dust density cannot fall with the same radial dependence as the late-type stellar density (§ VId); (2) there is no need to postulate the existence of extra luminosity sources at the galactic center, since those inferred from radio and near infrared observations provide sufficient power to account for the observed far infrared luminosity (see also § VIg).

f) Dust in the Galactic Center Region

The value of K (0.14 mag pc^{-1}) found from the model in the central 6 pc extrapolates to a visual extinction of 0.4 mag per parsec (Johnson and Borgman 1963) assuming the albedo of the grains is 0.5. The corresponding spatial density of dust is $\sim 4 \times 10^{-24}$ gm cm^{-3} (Aannestad and Purcell 1973). These values are somewhat more than one hundred times that in the solar neighborhood, whereas the stellar density in the galactic center is 10^7 times that in the solar neighborhood. The average electron density throughout Sgr A West is found from radio continuum observations to be $n_e = 10^3$ cm^{-3} (Ekers et al. 1975), implying an average gas-to-dust ratio of several hundred by mass within the central few parsecs of the Galaxy.

The visual extinction within 15 pc of the galactic center found from the model is 3.5 magnitudes. This is consistent with the conclusion of BN, based on their interpretation of the 2.2 μ radiation as starlight, that most of the 27 magnitudes of visual extinction to the galactic center are not located at the center, but rather are caused by intervening material in the line of sight to the source. Some authors (Andriesse and deVries 1976; Harvey, Campbell, and Hoffmann 1976) have suggested that the extinction occurring to and at the galactic center is substantially higher than the presently proposed value. The unique feature of the present analysis is that near infrared and far infrared data are used together to produce a self-consistent model of the galactic center region. We feel that this self-consistency serves to increase the plausibility of the picture of the galactic center which

emerges from the model and to strengthen the conclusion that the visual extinction close to the galactic center is small.

Within the central 3 pc of the Galaxy, there is only $\sim 1\ M_\odot$ of dust as opposed to $\sim 10^7\ M_\odot$ of stars. It is possible that the dust is provided by mass outflow from the stars. The arguments of Balick and Sanders (1974) suggest that the mass loss rate from late-type giant stars in this region is $\sim 5 \times 10^{-6}\ M_\odot$/yr; if 1 percent of the mass lost by stars is in the form of dust, the observed spatial density of dust will be built up in $\sim 10^7$ years.

It is an important conclusion of this paper that the spatial distribution of dust in the central 15 pc of the Galaxy is much more uniform than the distribution of the stars and gas, which are sharply concentrated toward the center. If the dust throughout the galactic center region is provided by mass loss from the stars, the dust distribution might be expected to be more similar to the stellar distribution than is observed. However, a dust distribution smoother than the stellar distribution could be produced in this case if the grains were selectively destroyed in, or expelled from, the high density central regions.

g) An Upper Limit to a Compact Optical and Ultraviolet Luminosity Source at the Galactic Center

It is of great interest to derive from the present data a reasonable numerical limit on hypothetical compact luminosity sources at the galactic center. The limit refers to sources other than those whose existence has been inferred from near infrared and radio observations (§II) which would contribute to heating the dust; that is, to sources

which radiate between 0.1 μ and 1 μ. As stressed in the previous sections, the model presented permits no significant presently unknown sources of luminosity in the galactic center. Since the model fits the data well in both the profiles of the far infrared luminosity and the energy distribution of the observed radiation, and since it is based on simple realistic assumptions about the grain properties and the distribution of dust, we believe that a conservative limit to such a hidden source of luminosity is $\sim 10^7\ L_\odot$.

Substantial changes must take place in the assumptions of the model if the strength of the hidden luminosity source is set well above this limit; for the purposes of discussion, a point source of $3 \times 10^7\ L_\odot$ will be considered. With the grain distribution and grain emissivity used in the best fit model calculation, such a hidden source would produce, among other effects, a factor of 10 too much luminosity in the central 3 pc of the Galaxy and a color temperature a factor of 1.5 times too high. To make the model consistent with the observations, it would be necessary at a minimum to (1) decrease the dust density in the central regions an order of magnitude while keeping the density higher in the outer regions; and (2) modify the grain emissivity within the central region to that of grey particles while leaving the properties of the outer grains unchanged. Because it would be necessary to make these artificial assumptions about the conditions in the galactic center region to fit the far infrared observations, we feel that a hidden central luminosity source greater than $10^7\ L_\odot$ can be safely ruled out.

VII. CONCLUSIONS

The region within 5' of the galactic center has a total far infrared luminosity of 4×10^7 $L_\odot$. All of the observed radiation can be interpreted as thermal emission from dust. The data presented on both color temperature and luminosity allow identification of the far infrared features with sources observed at other wavelengths, and the far infrared observations can be related in a simple, self-consistent way to near infrared, molecular line, and radio continuum observations of the galactic center.

The principal findings of the present experiment are:

(1) The far infrared emission from the galactic center region is radiated by dust heated both by the stellar distribution and by the ultraviolet sources which ionize the H II regions. Nonthermal emission does not contribute significantly to the far infrared luminosity of the galactic center region. The luminosity of any presently unidentified point source of 0.1 μ to 1 μ radiation at the galactic center is less than 10^7 $L_\odot$.

(2) The position of highest far infrared surface brightness is coincident with the peak of the stellar distribution and with the H II region Sgr A West. The far infrared luminosity of the central 1' of the Galaxy is 2.3×10^6 $L_\odot$. The spatial distribution of the far infrared surface brightness correlates principally with the location of stars and H II regions.

(3) All known H II regions in the area mapped appear as features in the far infrared data.

(4) There is no far infrared feature attributable to the supernova remnant Sgr A East.

(5) The molecular clouds near Sgr A make only a small contribution to the total far infrared luminosity of the region. They appear cold and dense in the far infrared. The galactic center is an example which illustrates that a strong far infrared source does not necessarily require the presence of a dense molecular cloud.

(6) The spatial distribution of the dust in the galactic center region is much more uniform than that of the stars. The whole region is remarkably dust free; within the central few parsecs of the Galaxy, the ratio by mass of dust to stars is 10^{-5} of that in the solar neighborhood, and the visual extinction across the central 10 pc of the Galaxy is only about 3 magnitudes. Mass loss by stars may account for the presence of this amount of dust. Our interpretation of the data favors a λ^{-1} dependence for the far infrared absorption efficiency of the grains out to $\sim$ 150 μ.

REFERENCES

Aannestad, P. A. 1975, Ap. J., 200, 30.

Aannestad, P. A. and Purcell, E. M. 1973, Ann. Rev. Astr. and Ap., 11, 309.

Alvarez, J. A., Furniss, I., Jennings, R. E., King, K. J., and Moorwood, A. F. M. 1974, in "H II Regions and the Galactic Centre," Proceedings of Eighth ESLAB Symposium, ed. by A. F. M. Moorwood (Neuilly-sur-Seine: ESRO) p. 69.

Andriesse, C. D. and de Vries, J. 1976, Astr. and Ap., 50, 99.

Balick, B. and Sanders, R. H. 1974, Ap. J., 192, 325.

Becklin, E. E. and Neugebauer, G. 1968, Ap. J., 151, 145.

Becklin, E. E. and Neugebauer, G. 1975, Ap. J. (Letters), 200, L71.

Becklin, E. E., Neugebauer, G., and Early, D. 1974, in "H II Regions and the Galactic Centre," Proceedings of Eighth ESLAB Symposium, ed. by A. F. M. Moorwood (Neuilly-sur-Seine: ESRO), p. 227.

Becklin, E. E., Matthews, K., Neugebauer, G., and Willner, S. P. 1977, (in preparation).

Bieging, J. H. 1976, Astr. and Ap., 51, 289.

Burbidge, G. R. and Stein, W. A. 1970, Ap. J., 160, 573.

Cameron, R. M., Bader, M., and Mobley, R. E. 1971, Appl. Opt., 10, 2001.

Campbell, M. F., Elias, J. H., Gezari, D. Y., Harvey, P. M., Hoffmann, W. F., Hudson, H. S., Neugebauer, G., Soifer, B. T., Werner, M. W., and Westbrook, W. E. 1976, Ap. J., 208, 396.

Ekers, R. D., Goss, W. M., Schwarz , U. J., Downes, D., and Rogstad, D. 1975, Astr. and Ap., 43, 159.

Elias, J. H., Gezari, D. Y., Hauser, M. G., Houck, J. R., Neugebauer, G., Werner, M. W., and Westbrook, W. E. 1977, (in preparation).

Fazio, G. 1976, private communication.

Furniss, I., Jennings, R. E., and Moorwood, A. F. M. 1974, in "H II Regions and the Galactic Centre," Proceedings of Eighth ESLAB Symposium, ed. by A. F. M. Moorwood (Neuilly-sur-Seine: ESRO), p. 61.

Harper, D. A. 1974, Ap. J., 192, 557.

Harvey, P. M., Campbell, M. F., and Hoffmann, W. F. 1976, Ap. J. (Letters), 205, L69.

Hoffmann, W. F. and Frederick, C. L. 1969, Ap. J. (Letters), 155, L9.

Hoffmann, W. F., Frederick, C. L., and Emery, R. J. 1971, Ap. J. (Letters), 164, L23.

Ingersoll, A. P., Münch, G., Neugebauer, G., and Orton, G. S. 1976, "Jupiter," ed. T. Gehrels, University of Arizona Press, p. 197.

Johnson, H. L. and Borgman, J. 1963, B.A.N., 17, 115.

Liszt, H. S., Sanders, R. H., and Burton, W. B. 1975, Ap. J., 198, 537.

Low, F. J. and Aumann, H. H. 1970, Ap. J. (Letters), 162, L79.

Mezger, P. G. 1974, Proceedings of the ESO/SRC/CERN Conference on Research Programmes for the New Large Telescopes, Geneva, ed. by A. Reiz, p. 79.

Neugebauer, G., Becklin, E. E., Beckwith, S., Matthews, K., and Wynn-Williams, C. G. 1976, Ap. J. (Letters), 205, L139.

Olthof, H. 1975, Ph.D. Thesis, Kapteyn Astronomical Institute, Groningen, The Netherlands.

Osterbrock, D. E. 1974 , in "Astrophysics of Gaseous Nebulae," (W. H. Freeman and Company).

Panagia, N. 1973, A. J., 78, 929.

Pauls, T., Downes, D., Mezger, P. G., and Churchwell, E. 1976, Astr. and Ap., 46, 407.

Purcell, E. M. 1969, Ap. J., 158, 433.

Rieke, G. H., Harper, D. A., Low, F. J., and Armstrong, K. R. 1973, Ap. J. (Letters), 183, L67.

Sanders, R. H., and Lowinger, T. 1972, A. J., 77, 292.

Scoville, N. Z. 1972, Ap. J. (Letters), 175, L127.

Scoville, N. Z., Solomon, P. M., and Jefferts, K. B. 1974, Ap. J. (Letters), 187, L63.

Solomon, P. M., Scoville, N. Z., Penzias, A. A., Wilson, R. W., and Jefferts, K. B. 1972, Ap. J., 178, 125.

Telesco, C. M. and Harper, D. A. 1975 BAAS, 7, 530.

Werner, M. W., Gatley, I., Harper, D. A., Becklin, E. E., Lowenstein, R. F., Telesco, C. M., and Thronson, H. A. 1976, Ap. J., 204, 420.

Werner, M. W., Becklin, E. E., and Neugebauer, G. 1977, Science, (in press).

Westbrook, W. E., Werner, M. W., Elias, J. H., Gezari, D. Y., Hauser, M. G., Lo, K. Y. , and Neugebauer, G. 1976, Ap. J., 209, 94.

FIGURE CAPTIONS

Fig. 1 The arrangement of filters, field optics, and detectors inside the dewar. R1 is CsBr, R2 is CaF_2 backed by sapphire; B1 is a 22-35 μ interference filter, B2 is KRS-5, B3 is CaF_2 backed by sapphire.

Fig. 2 The measured spectral response for each of the three channels.

Fig. 3 (a) Map of the galactic center region at 2.2 μ. The contour interval is equivalent to 3 Jy into a 1' diameter beam. (1 Jy = 10^{-26} W m^{-2} Hz^{-1}). The dashed contour is at half this level. The cross in Figs. 3a-3d indicates the position of Sgr A West. Note that the angular resolution of this 2.2 μ map is slightly less than that of the far infrared maps shown in Figs. 3b, 3c, and 3d.

(b) Map of the galactic center region at 30 μ. The diagonal dashed lines indicate the area mapped. The contour interval is equivalent to 1.2 x 10^3 Jy into a 1' diameter beam.

(c) Map of the galactic center region at 50 μ. The contour interval is equivalent to 1.1 x 10^3 Jy into a 1' diameter beam.

(d) Map of the galactic center region at 100 μ. The contour interval is equivalent to 600 Jy into a 1' diameter beam.

Fig. 4 (a) Map of the far infrared luminosity of the galactic center region obtained by integration over the three wavelength bands of the present experiment. The contour interval is equivalent

to 1.0×10^{-10} W m^{-2} into a 1' diameter beam. The dashed contour is at half this level. The cross in Figs. 4a, 4b, and 4d indicates the position of Sgr A West.

(b) Map of the 50 μ - 100 μ color temperature derived from the data of Figs. 3c and 3d. The contours are labelled in °K.

(c) Map of the 10.7 GHz radio continuum emission from the galactic center region from Pauls et al. (1976). The contour levels are at 5, 10, 20, 40, 60, 80, and 100; the contour unit is 0.47^{o}K main beam brightness temperature. The letters W and E indicate the positions of Sgr A West and East, respectively. The positions of the H II regions G0.07+0.04, G0.01+0.02, and G0.01-0.12 are also shown.

(d) Map of the ^{12}CO emission near the galactic center from Solomon et al. (1972). The dashed contours show features between 45 and 65 km/sec and the solid contours show features between 15 and 35 km/sec. The contours are labelled in units of peak antenna temperature.

Fig. 5 Normalized scans through the galactic center along and across the galactic plane. The far infrared data are taken from the contour maps of Figs. 3 and 4. The 2 μ profile is from Figure 5 of Becklin and Neugebauer (1968). The units along the scan direction are arcminutes. The major axis scans are in the direction of increasing galactic longitude; the minor axis scans are in the direction of increasing galactic latitude.

Fig. 6 The 30 μ to 1 mm energy distribution of the central 1' of the Galaxy. The present data have been corrected for beam size and shape effects. The 2 σ upper limit at 350 μ is from Rieke et al. (1973). The solid line indicates the energy distribution predicted by the model of §VI. The dashed line indicates the expected level of free-free radiation extrapolated from radio continuum observations (Pauls et al. 1976).

Fig. 7 The luminosity of the region around the galactic center observed over a range of diaphragm diameters. The filled circles are the observed far infrared and submillimeter luminosity, the solid line shows the stellar luminosity inferred from 1-3 μ observations, and the crosses show the values of E_M, the minimum luminosity of the ionizing sources, inferred from radio continuum observations. The far infrared and submillimeter data are from Harvey, Campbell, and Hoffmann (1976), this paper, Low and Aumann (1970), and Olthof (1975). The stellar luminosity is from BN, and the values of E_M are from Ekers et al. (1975) and Mezger (1974).

Fig. 8 (a) The observed far infrared surface brightness as a function of distance from the galactic center along the galactic plane (filled squares) and that predicted by the model for the case K = 0.14 mag pc^{-1} at $r \leq 3$ pc and K = 0.07 mag pc^{-1} at $r > 3$ pc. Curves 1 and 2 show respectively the contributions from the point source of luminosity 3×10^6 $L_\odot$ and from the stellar distribution (see text).

(b) Curve 1 shows the effect of increasing K, and curve 2 of decreasing K, by a factor of three from the value of Fig. 8a. Curve 3 shows the effect of a gradient in K with approximately the same dependence on distance from the galactic center as that of the stellar density.

Fig. 9 The observed 50 μ to 100 μ color temperature (filled triangles) is compared with that predicted by two forms of the far infrared grain absorption efficiency for the case shown in Fig. 8a. The curve corresponds to a far infrared grain absorption efficiency $Q \propto \lambda^{-1}$. The dashed curve corresponds to $Q \propto \lambda^{-2}$ (see text). Uncertainties in the flux calibration could systematically alter the observed color temperatures by up to $\pm 15^{o}$K.

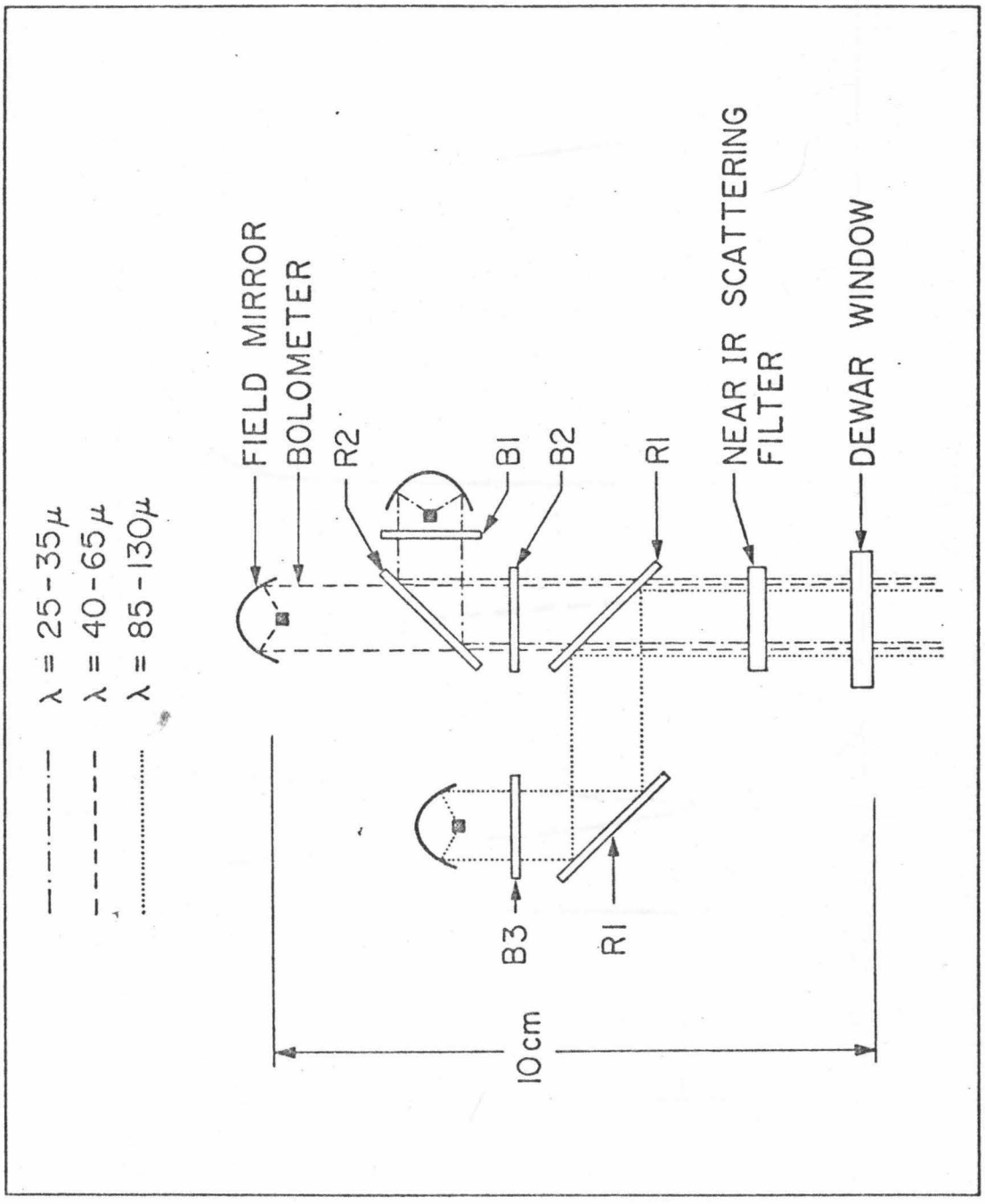
λ = 25-35μ
λ = 40-65μ
λ = 85-130μ
FIELD MIRROR
BOLOMETER
R2
B1
B2
R1
NEAR IR SCATTERING FILTER
DEWAR WINDOW
B3
R1
10cm

Figure 1

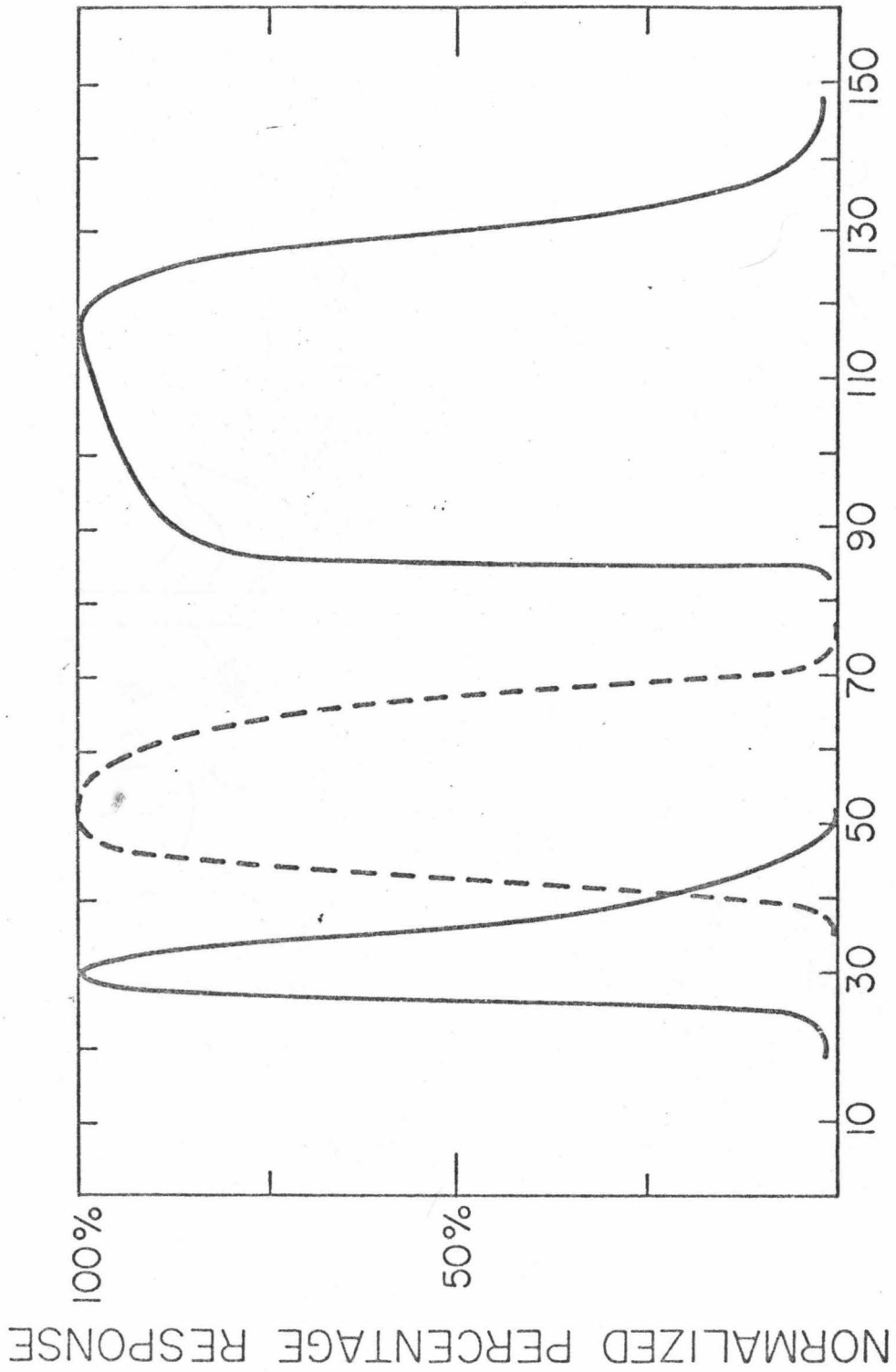
NORMALIZED PERCENTAGE RESPONSE
100%
50%
10
30
50
70
90
110
130
150
λ (μ)

Figure 2

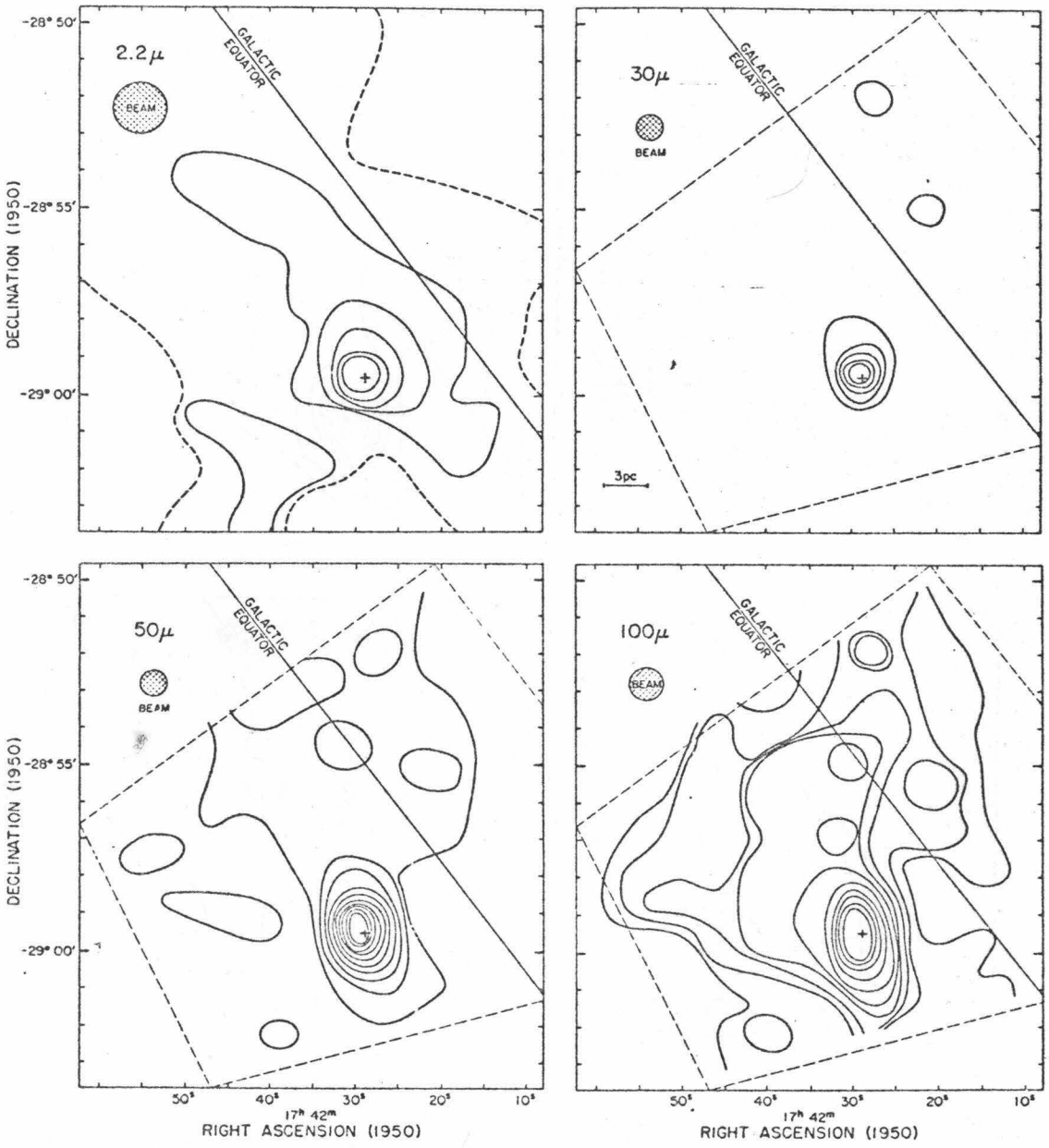
2.2μ
BEAM
GALACTIC EQUATOR
30μ
BEAM
GALACTIC EQUATOR
3pc
50μ
BEAM
GALACTIC EQUATOR
100μ
BEAM
GALACTIC EQUATOR
-28° 50'
-28° 55'
-29° 00'
DECLINATION (1950)
50s
40s
30s
20s
10s
17h 42m
RIGHT ASCENSION (1950)

Figure 3

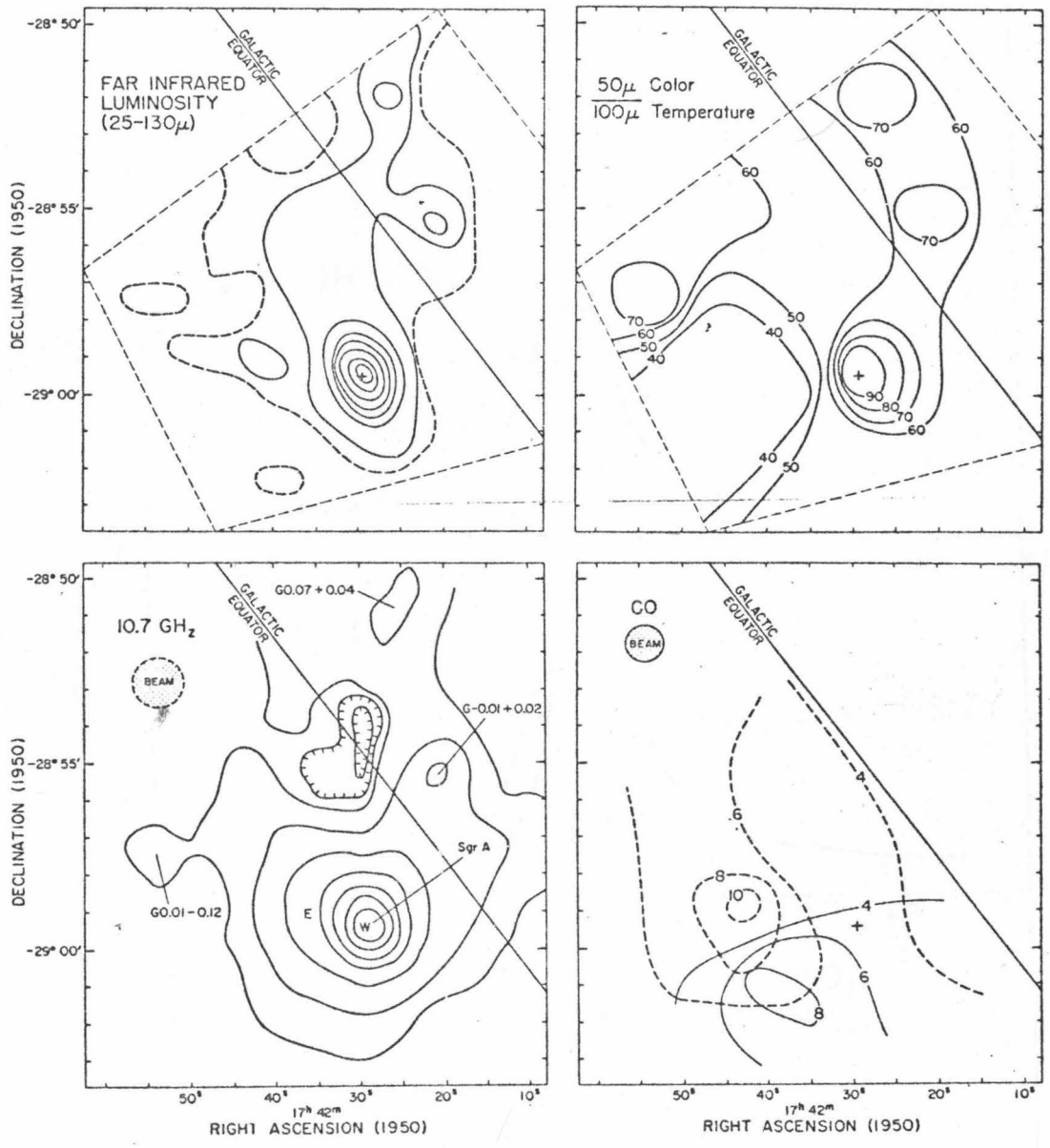
FAR INFRARED
LUMINOSITY
(25-130μ)
GALACTIC EQUATOR
50μ Color
100μ Temperature
10.7 GHz
BEAM
G0.07 + 0.04
G-0.01 + 0.02
Sgr A
E
W
G0.01 - 0.12
CO
DECLINATION (1950)
-28° 50'
-28° 55'
-29° 00'
17h 42m
RIGHT ASCENSION (1950)

Figure 4

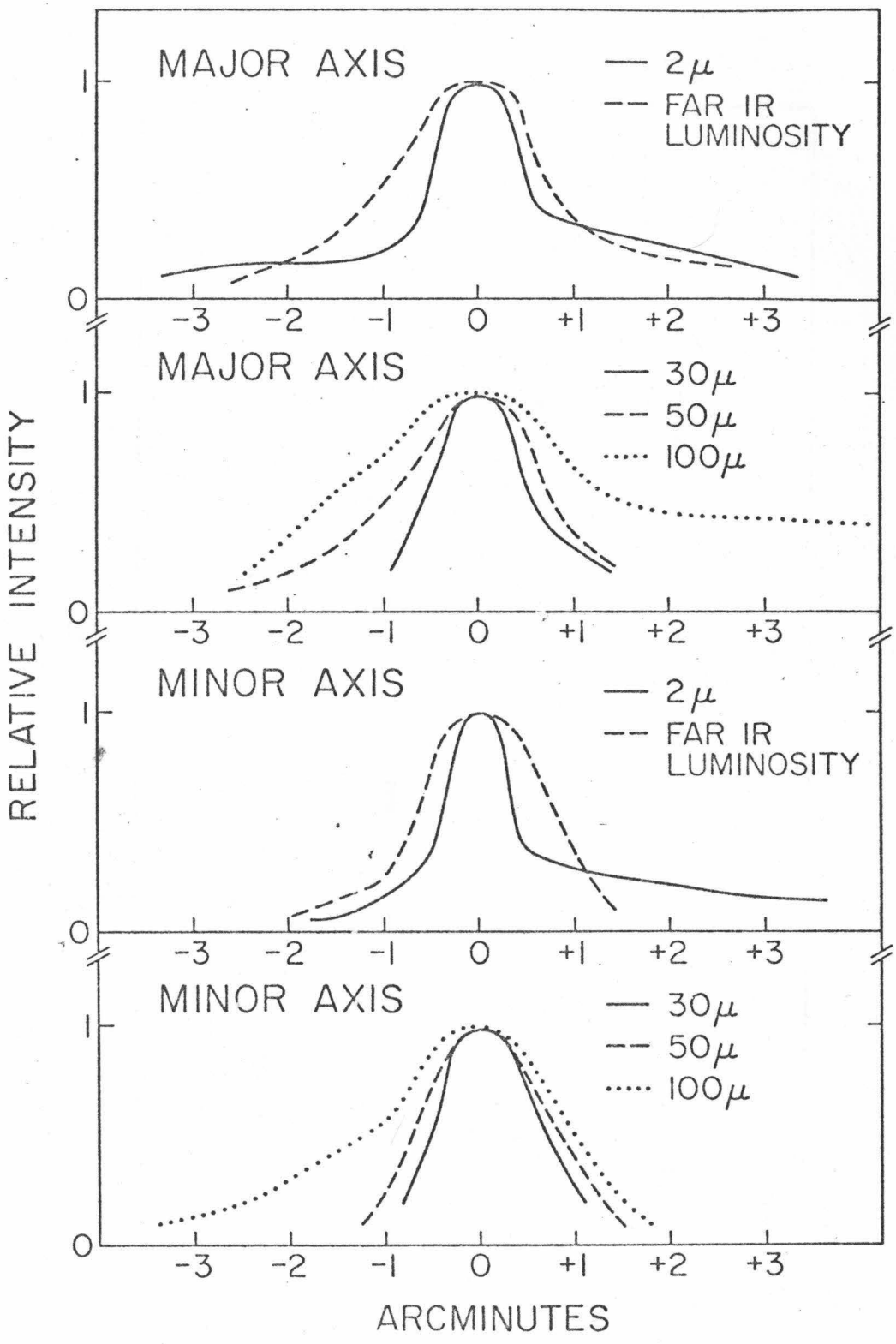
MAJOR AXIS
2μ
FAR IR LUMINOSITY
MAJOR AXIS
30μ
50μ
100μ
MINOR AXIS
2μ
FAR IR LUMINOSITY
MINOR AXIS
30μ
50μ
100μ
RELATIVE INTENSITY
ARCMINUTES
-3 -2 -1 0 +1 +2 +3
1
0

Figure 5

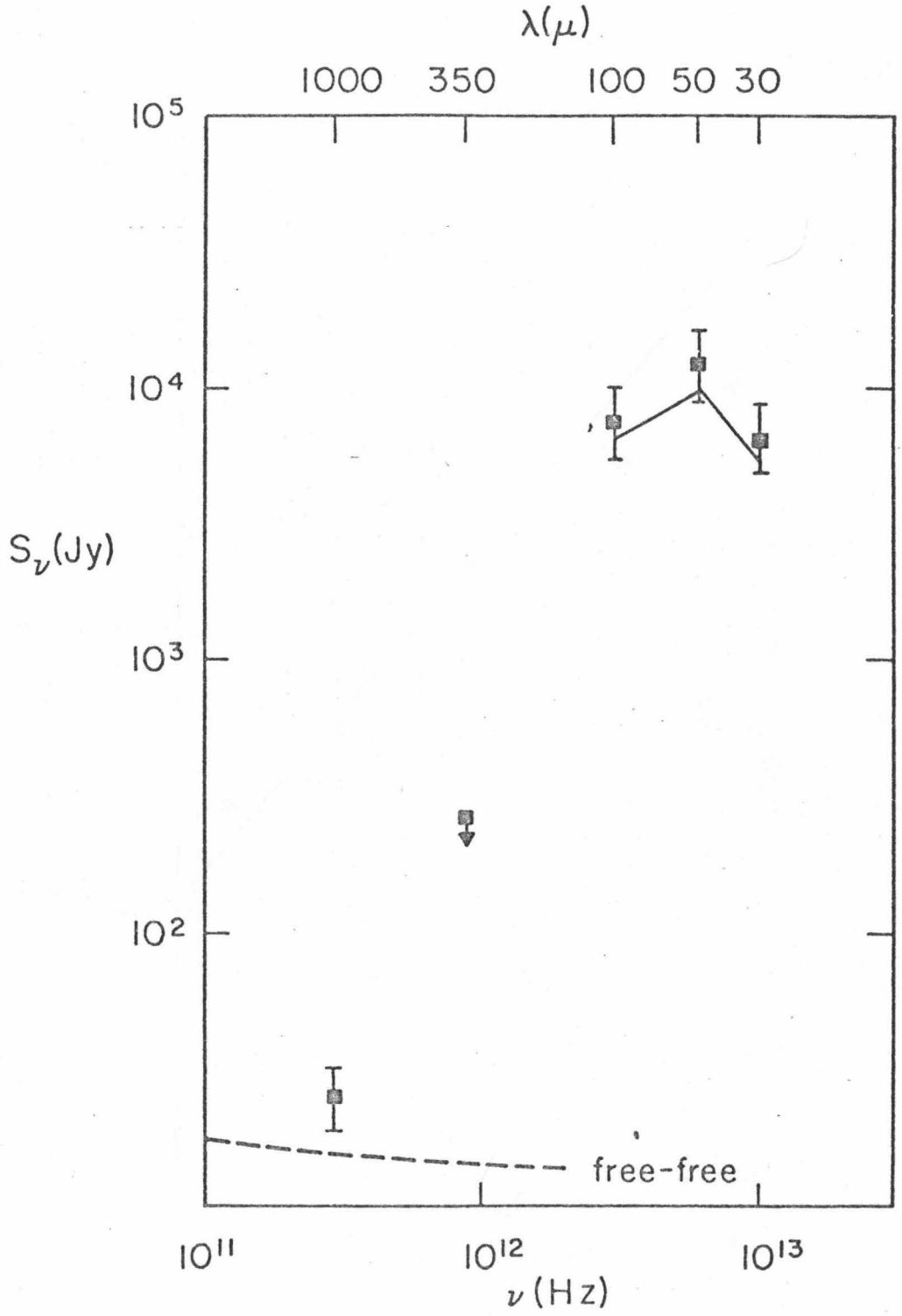
λ(μ)
1000
350
100
50
30
10^5
10^4
10^3
10^2
S_ν(Jy)
free-free
10^11
10^12
10^13
ν(Hz)

Figure 6

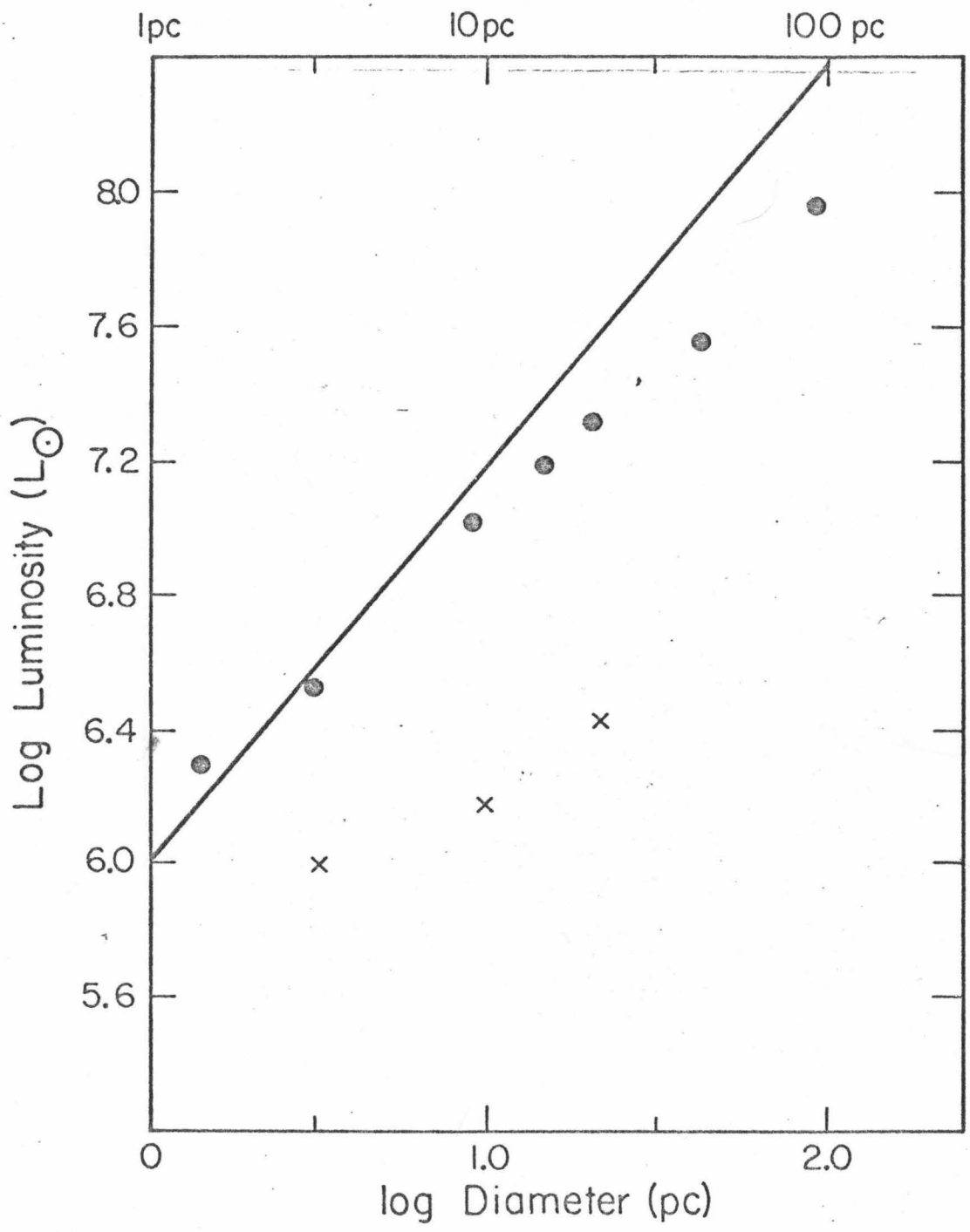
1pc
10pc
100 pc
8.0
7.6
7.2
6.8
6.4
6.0
5.6
Log Luminosity ($L_\odot$)
0
1.0
2.0
log Diameter (pc)

Figure 7

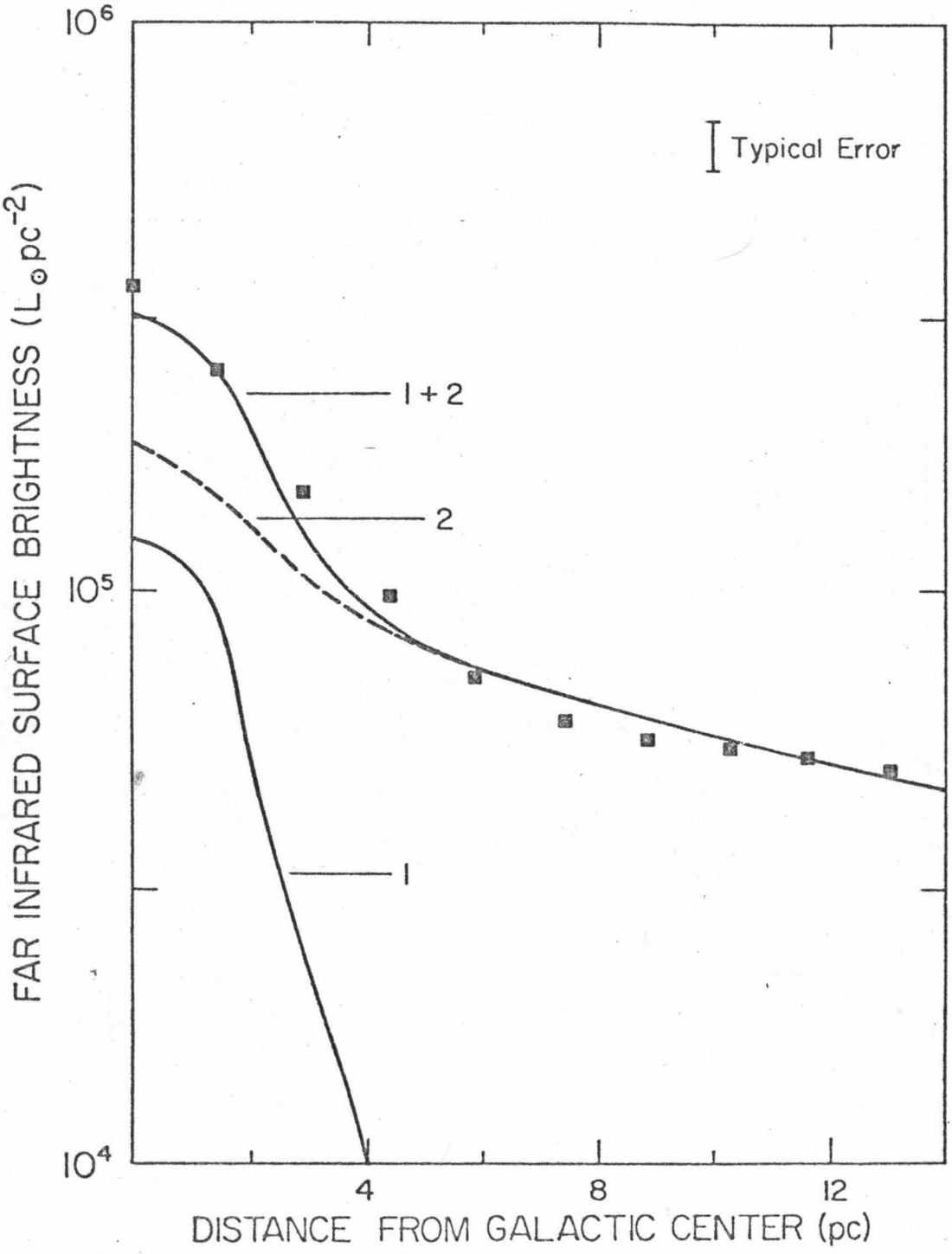
10^6
10^5
10^4
FAR INFRARED SURFACE BRIGHTNESS ($L_\odot pc^{-2}$)
Typical Error
1+2
2
1
4
8
12
DISTANCE FROM GALACTIC CENTER (pc)

Figure 8a

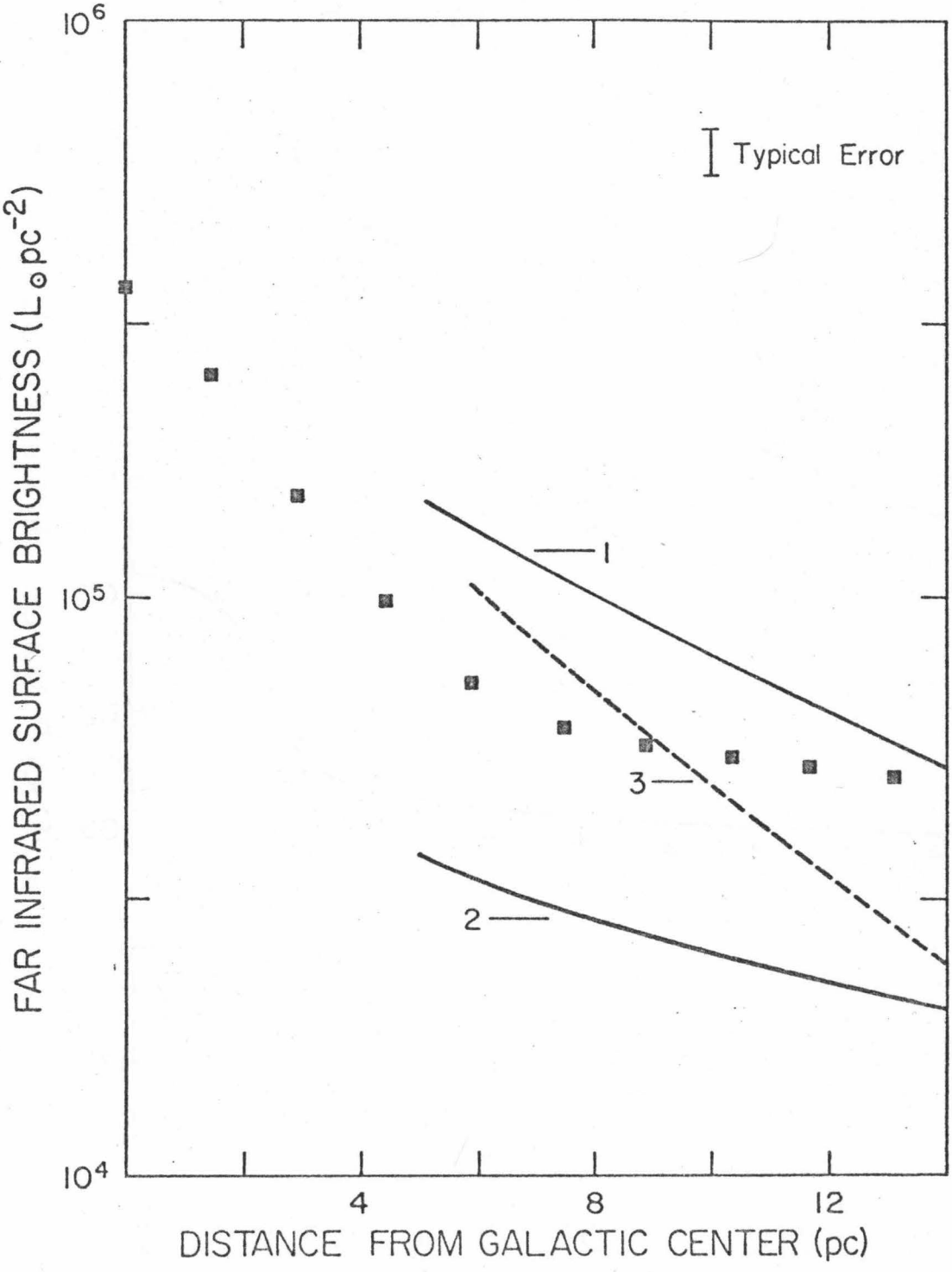
10^6
10^5
10^4
FAR INFRARED SURFACE BRIGHTNESS ($L_\odot pc^{-2}$)
Typical Error
1
2
3
4
8
12
DISTANCE FROM GALACTIC CENTER (pc)

Figure 8b

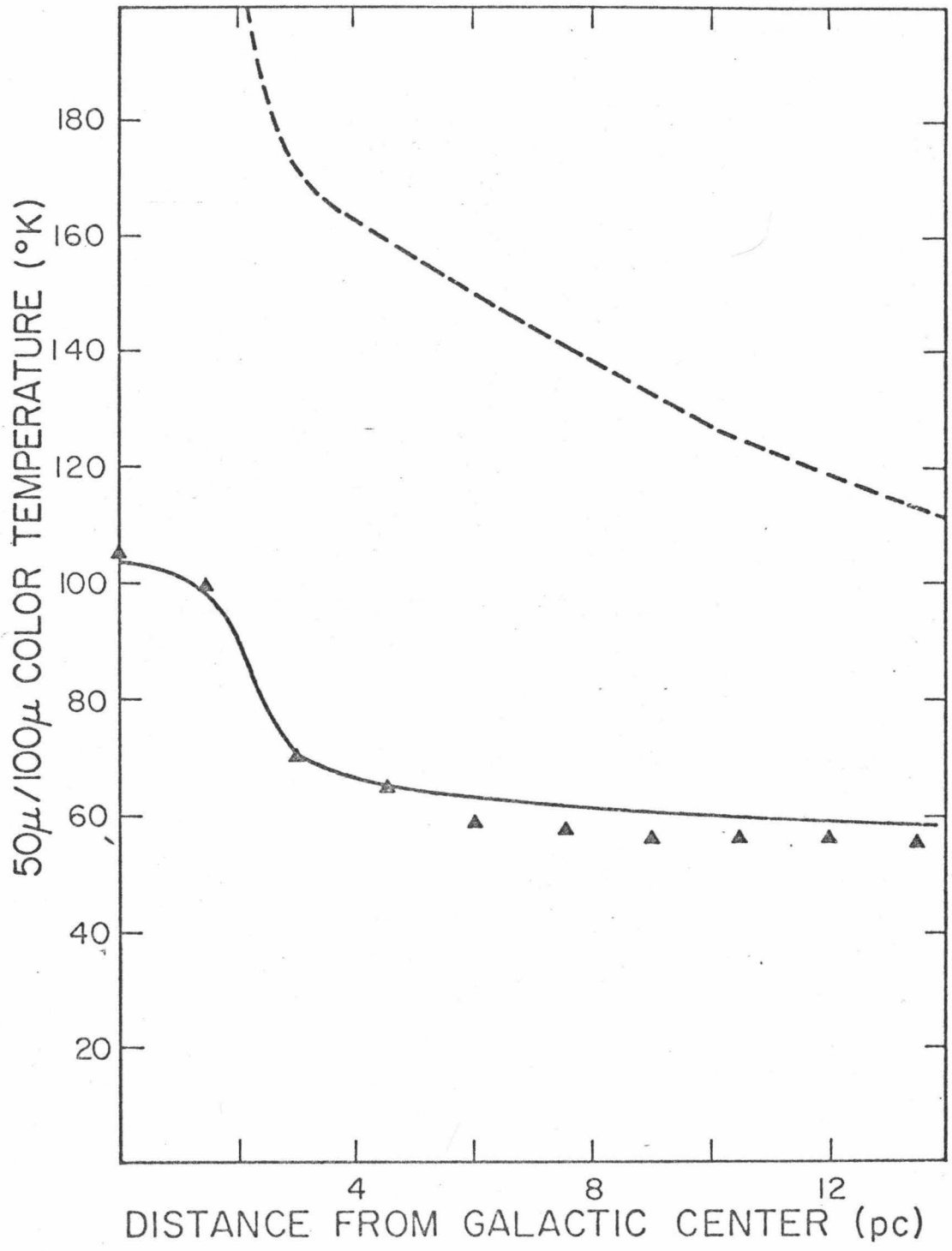
180
160
140
120
100
80
60
40
20
50μ/100μ COLOR TEMPERATURE (°K)
4
8
12
DISTANCE FROM GALACTIC CENTER (pc)

Figure 9

CHAPTER 2

H II REGIONS NEAR THE GALACTIC CENTER

I. INTRODUCTION

Within a few hundred parsecs of the galactic center there exists a highly complex distribution of H II regions and molecular clouds (for a comprehensive review see Oort 1977). Although little is understood of the nature of these H II regions, and in particular the source of ionization is unknown, it has been suggested by many authors that these H II regions surround early type stars newly formed in the molecular clouds (e.g., Martin and Downes 1972; Mezger, Churchwell and Pauls 1974; Genzel, Downes and Bieging 1976).

A straightforward method of studying the gross energetics of H II regions is provided by far infrared observations, because, typically, almost all of the luminosity associated with the region is ultimately absorbed by dust and thermally re-radiated. In the previous chapter (referred to hereafter as "Paper I") we reported far infrared* mapping of a

---

*The term "far infrared" is used here to denote wavelengths $25 < \lambda < 130$ μm.

10' diameter region around Sgr A with 1' angular resolution. Here we add far infrared maps of the Sgr B2/G0.5+0.0 region and measurements of the source Sgr C made with the same experiment. There are nine discrete radio sources within the regions mapped which can be identified with H II regions because they show both a flat radio continuum spectrum and radio recombination line radiation; these have all been detected in the far infrared. Discussion of these sources is the main subject of this paper. By comparing the observed properties of the galactic center H II regions both with each other and with the properties of well-studied spiral arm H II regions where

stars are forming, we hope to make some modest beginnings towards understanding star formation in the galactic center.

II. OBSERVATIONS

The observations reported here were made at an altitude of 12.3 km from the NASA 0.9 m airborne telescope (Cameron, Bader and Mobley 1971). The instrumentation, observing techniques, and data reduction are discussed in detail in Paper 1. Briefly, the experiment measures the flux from the same $\sim$ 1' field of view simultaneously in well-defined bands at three wavelengths, namely 30 μm ($\Delta\lambda$ = 10 μm), 50 μm ($\Delta\lambda$ = 25 μm), and 100 μm ($\Delta\lambda$ = 45 μm). Guiding of the telescope is achieved by optical viewing of stars in the focal plane through a dichroic mirror; the resulting positional accuracy is ± 20". Maps are constructed by sampling a grid with 30" spacing between adjacent points; the integration time per point is 10 seconds. The beam profiles were mapped on Saturn, the diameter of which was 17" at the time of observation. The beams were approximately Gaussian in shape, and the full width at half maximum of the beam was 40" at 30 μm and 50 μm, and 55" at 100 μm. For convenience throughout this paper, fluxes have been corrected to that which would be measured in a 1' beam under the assumption that the sources have uniform surface brightness over 1'. Flux calibration was achieved by observations of Jupiter, for which the far infrared energy distribution is assumed to be given by a model based on measurements from Pioneer 10 (Ingersoll *et al.* 1976). The measured beam profile has been integrated over the planet disk to calculate the flux reaching the detector at each wavelength.

III. RESULTS

The mechanism for the observed far infrared radiation will be assumed to be thermal emission from dust. Detailed justification of this point is given in Paper 1. The three most important quantities which have been derived from the far infrared data and are used in physical interpretation are the far infrared luminosity, color temperature, and optical depth of emission. A fourth derived quantity discussed in this paper is the infrared excess of an H II region; this quantity describes the far infrared luminosity of an H II region relative to its radio continuum flux. We define these four quantities and discuss the assumptions made in their derivation and use in the Appendix.

a) Appearance of the Maps

In Paper 1 we presented and discussed in detail far infrared maps of a 10' diameter region around Sgr A. There are four H II regions seen in those maps: Sgr A West, G0.07+0.04, G0.01+0.02 and G0.01-0.12. Each of these H II regions appears, relative to nearby locations in the galactic plane, as a position of enhanced luminosity and color temperature with no appreciable increase in the optical depth of emission.

In Figures 1(a) and 1(b) we present 50 μm and 100 μm maps of the portion of the galactic plane between G0.5+0.0 and Sgr B2. Although individual sources were detected at 30 μm, the signal-to-noise ratio at that wavelength was not sufficient to allow construction of a map. Figure 1(c) shows the mean color temperature and optical depth of emission each averaged over $\sim$ 2' regions; these quantities are displayed superposed on the 50 μm map of Figure 1(a). The dashed lines in Figure 1(c) are contours of $\int N(^{13}CO)dV$ (Scoville, Solomon and Penzias 1975); if the

^{13}CO emission is optically thin these contours indicate the molecular column density through the cloud. Figure 1(d) is a 10.7 GHz radio continuum map with 77" resolution (Downes, 1974) included for comparison purposes.

There is an obvious correlation between the radio continuum and far infrared emission in Figure 1. In particular, one can easily identify emission from the regions Sgr B2, G0.6+0.0 (which is component 2 of Martin and Downes 1972) and both north and south components of G0.5+0.0 (Downes 1974). Additionally, the general extended emission from the galactic plane between these sources has roughly the same spatial distribution at radio and infrared wavelengths. There is, however, a weak feature in the radio continuum map 3' south of Sgr B2 which has no infrared counterpart.

A very striking feature of the infrared maps of Figure 1 is the large range of temperatures observed, which vary monotonically across the region from $\sim$ 30 K at Sgr B2 to $\sim$ 90 K at G0.5+0.0. The corresponding far infrared optical depth of emission decreases from about unity at Sgr B2 to 0.01 at G0.5+0.0, indicating large changes in the column density of radiating dust.

b) Scans of Sgr C

Sgr C (Hoffmann, Frederick and Emery 1971; Alvarez et al. 1974; Brown and Broderick 1973) is located in the galactic plane at negative longitude. The projected distance of Sgr C from the galactic center is about $0^{\circ}.5$; that is, Sgr C and G0.5+0.0 are symmetrically located about the galactic center. The observations of Sgr C are very limited; scans through the peak of the source in each of two orthogonal directions show it to be comparable in size, surface brightness, and color temperature to G0.5+0.0.

c) Properties of the H II Regions

All individual H II regions present in the 77" resolution, 10.7 GHz radio continuum maps are seen in the far infrared maps, and except in the vicinity of Sgr B2 the H II regions are characterized by local increases in luminosity and color temperature, but not in optical depth of emission.

The observed far infrared fluxes for the central 1' of each of the nine H II regions are presented in Table 1, together with the resulting luminosity, color temperature, and optical depth of emission derived as described in the Appendix. The luminosity of each region is equivalent to that of several early O stars. Also included in Table 1 are the radio continuum flux (Pauls et al. 1976; Downes 1974; Kapitzky and Dent 1974) and the infrared excess. Values for the infrared excess in spiral arm H II regions are in the range 3-20 (Jennings 1975; Furniss, Jennings and Moorwood 1974). The galactic center H II regions all have an infrared excess in this range.

The energy distributions of the sources Sgr B2, G0.6+0.0 and G0.5+0.0 are plotted in Figure 2. These energy distributions clearly illustrate the large range of temperatures of the present sample of H II regions.

IV. NOTES ON INDIVIDUAL SOURCES

a) Sgr B2

The thermal radio emission from Sgr B2 (G0.7-0.1) has been resolved interferometrically into several compact H II regions each less than 10" in diameter and rather like M42 (Martin and Downes 1972); there is also a more extended diffuse component $\sim 4'$ in extent (Figure 1d). Intimately associated with these H II regions is the densest molecular cloud in the

Galaxy, with hydrogen column densities of 10^{24} cm^{-2} (an average volume density of 5×10^4 H_2 cm^{-3}) in the 2' diameter core (Scoville, Solomon and Penzias 1975); the total spatial extent of the cloud is about 15'.

The far infrared emission from Sgr B2 is strongly peaked at the position of the thermal radio peak (see Fig. 1); this is also the position of greatest continuum emission at 350 μm and 1 mm and of the core of the molecular cloud (Righini et al.1975; Westbrook et al.1976; Scoville, Solomon, and Penzias 1975). The far infrared luminosity (25-130 μm) of the central 1' of Sgr B2 is 2.7×10^6 $L_\odot$, and of the central 3!5, by spatial integration, 6×10^6 $L_\odot$, in agreement with previous measurements (Low and Aumann 1970; Harper 1974; Harvey, Campbell, and Hoffmann 1977). This luminosity is not unusually large for a galactic H II region/molecular cloud complex (Harvey, Hoffmann, and Campbell 1975; Thronson 1977). What is extraordinary about Sgr B2 as compared with similar regions is the near equality of observed far infrared color and brightness temperatures; this implies that the source is optically thick in the far infrared. This had been previously suggested from far infrared and 350 μm observations, and to explain the failure of high spatial resolution (17") 53 μm mapping to resolve the individual H II regions (Harper 1974; Rieke et al. 1973; Harvey, Campbell, and Hoffmann 1977; Righini et al. 1975). Because the source is optically thick, it is not possible to derive the physical grain temperatures in the center of the cloud directly, but the relative compactness of the 50 μm source with respect to the 100 μm source shows clearly that temperature gradients are present within the cloud, as is expected in a region heated by embedded luminosity

sources. Such temperature gradients are observed directly in far infrared observations of less heavily dust obscured regions, as, for example, in OMC1 (Werner et al. 1976).

The physical complexity of Sgr B2 precludes the construction of a detailed quantitative model of the source, but a comparison with the observed parameters of the giant H II region/molecular cloud complex W51 is instructive. The distance, far infrared luminosity, and radio flux of W51 are all similar to those of Sgr B2; the major difference between the sources is that Sgr B2 appears cold and optically thick in the far infrared, while W51 (Harvey, Hoffmann, and Campbell 1975; Thronson 1977) appears hot (color temperature = 75 K) and optically thin ($\tau \approx 0.1$ at 50 μm). We attribute this difference in appearance solely to the great column density of dust in the Sgr B2 molecular cloud. If a source like W51 were enclosed in a dense dust cloud whose 100 μm optical depth is near unity, then the observed properties of this source would be very much like those of Sgr B2.

A model of this type is consistent with all observations of Sgr B2 to date. The high dust densities implied are known to exist from molecular and 1 mm continuum studies. The column density of dust and distribution of 100 μm surface brightness conform with the picture presented by Scoville, Solomon and Penzias (1975) based on a similar physical model for the interpretation of their molecular observations. The extreme faintness of Sgr B2 at wavelengths of 2-20 μm (Becklin et al. 1977) is naturally explained.

In Figure 1(c) we compare the far infrared optical depths of emission with the molecular column density (contours of $\int N(^{13}CO)dV$) for the region of the galactic plane from Sgr B2 and G0.5+0.0. The correlation between

these quantities suggests that the dust radiating in the far infrared is well mixed with the gas in the molecular cloud.

Molecular observations of Sgr B2 have shown that the gas temperature is $\sim$ 20 K throughout most of the cloud, but rises in a small region of the core (Scoville, Solomon, and Penzias 1975). A comparable range of grain temperatures is suggested by the far infrared observations. Therefore, the observations are not inconsistent with the hypothesis that the gas and dust temperatures are coupled in the molecular cloud.

In summary, we find that for Sgr B2: (1) The source appears spatially extended, cold, and dense in the far infrared. (2) The H II regions lie deep in the molecular cloud as seen from the earth. (3) The grain temperature increases in the center of the cloud. (4) The dust and gas temperatures within the molecular cloud are similar.

b) G0.5-0.0 and G0.6-0.0

These H II regions are located in the galactic plane near Sgr B2. This segment of the plane has a particularly interesting appearance in the far infrared, because the inferred column density of radiating dust varies monotonically through more than two orders of magnitude in a projected distance of 30 pc, and the corresponding color temperatures vary from 30 K to 90 K. These phenomena are related to the distribution of molecular clouds; Figure 1(c) displays molecular column densities throughout the region, and shows clearly that G0.5-0.0 is outside the bulk of the Sgr B2 molecular cloud, while G0.6-0.0 is partially embedded in it. The appearance of this portion of the galactic plane is like that of regions of star formation in the spiral arms of the Galaxy (e.g., Israel 1976; Elmegreen and Lada 1977) in terms of relative spatial location and age, size, clustering, and disposition of the H II regions with respect to the molecular clouds.

c) G0.07+0.04

This very luminous source is located at a projected distance of 8' (24 pc) from the galactic nucleus. In a far infrared luminosity map of the region with 1' x 1!5 resolution, G0.07+0.04 is shown as having half the luminosity of Sgr A in a single beam (Fazio, private communication) which is consistent with our result. This H II region has the highest infrared excess in our sample. This is suggestive of the presence of a large source of non-ionizing radiation in this region; in spiral arm H II region complexes this often signifies the presence of newly formed or forming stars (Werner, Becklin and Neugebauer 1977). Therefore, G0.07+0.04 may represent a region of current star formation in the vicinity of the galactic center, and should be studied in more detail.

d) Sgr A

The H II region Sgr A is located at the position of highest stellar density in the Galaxy (Oort 1977), and so there has been a great deal of speculation as to its nature. Sgr A is remarkable amongst the present sample of H II regions for its high color temperature and low infrared excess (Table 1; Furniss, Jennings, and Moorwood 1974). This low value of the infrared excess may be attributable to the nature of the source(s) which ionize Sgr A, or it may simply imply a low dust density in Sgr A so that luminosity is absorbed and reradiated in the far infrared over a region larger than 1' in extent.

e) Sgr C

The limited far infrared observations of Sgr C show it to be rather similar to G0.5-0.0 in its size, color temperature, and luminosity. Scans through the source show that Sgr C does not have a strong central condensation of surface brightness; comparison of the far infrared luminosity measured with a 1' beam, 3.8×10^5 $L_\odot$ (Table 1) to that measured with a 5'.6 beam, 4.2×10^6 $L_\odot$ (Alvarez et al. 1974) confirms that the surface brightness is rather uniform across a 5' diameter region.

The scans through Sgr C show no evidence for temperature variations in the source. The far infrared optical depth of emission is low (Table 1) indicating that this source is not embedded in a dense molecular cloud. Therefore Sgr C looks in all regards like the giant H II region G0.5-0.0, and not at all like Sgr B2. It has long been known that the distribution of molecular clouds and H II regions in the galactic center region is extremely asymmetric, with the vast majority being at positive longitudes. The similarity of Sgr C to G0.5-0.0 is consistent with this apparent absence of extremely young regions at negative galactic longitudes.

V. DISCUSSION

a) The Nature of the H II Regions

The major result of this study of the galactic center region is that each of the individual H II regions detected in comparable angular resolution radio studies is seen in the far infrared, and at about the level expected from the radio brightness. This suggests immediately that none of these regions is a radically new type of object, but is, at least superficially, like other H II regions in the Galaxy. Furthermore, the local increase in both luminosity and color temperature seen at the positions of most of these H II regions demands that each H II region contains its own source of luminosity, which is presumably also the source of ionization. The nature of this source of ionization and luminosity is important, for if it is the case that the majority of galactic center H II regions is powered by early type stars, then a high rate of star formation is implied (Mezger and Smith 1977).

Table 1 lists the observed properties of the nine H II regions, and the derived quantities of far infrared luminosity, color temperature, optical depth, and infrared excess (see Appendix). Each of these parameters is within the range typically observed for spiral arm H II regions (e.g., Furniss, Jennings, and Moorwood 1974) where the source of ionization and luminosity is known to be recently formed early type stars. Therefore the observed properties of H II regions near the galactic center are similar to those of spiral arm H II regions; the simplest explanation of this fact is that we are observing similar phenomena in both cases, that is, that the galactic center is a region of recent, intense star formation.

The values determined for the infrared excess for the H II regions other than Sgr A further imply that, like spiral arm H II regions, these galactic center objects are surrounded by regions where the dust density is high enough that the optical and near ultraviolet radiation of the exciting stars(s) is absorbed and converted to far infrared in the immediate vicinity of the H II region. For spiral arm H II regions, this is a natural result of the fact that the H II regions are generally associated with molecular clouds. A similar association with molecular clouds may be indicated for the galactic center H II regions by the present results; of course such an association is shown directly by the data for G0.5-0.0, G0.6-0.0, and Sgr B2 in Figure 1.

The low value of the infrared excess for Sgr A suggests that the dust density around this H II region may be lower than near the other H II regions, so that the stellar photons can escape from the immediate vicinity of Sgr A. This result is consistent with the low and spatially uniform value for the dust density derived for the central region of the Galaxy in Paper 1. Thus, the differences in far infrared appearance between Sgr A and the other H II regions may be due largely to the environment of the H II region and not to the nature of the ionizing sources.

b) Morphology of the Galactic Plane between $\ell = 0^{\circ}.5$ and $\ell = 0^{\circ}.7$

As we have pointed out in §IV(b), the portion of the galactic plane between G0.5-0.0 and Sgr B2 is strikingly similar to regions of star formation in the spiral arms of the Galaxy. The chain of H II regions stretching along the galactic plane appear successively more compact, more deeply dust embedded, and presumably younger. In spiral arms this

type of morphology has been interpreted (Elmegreen and Lada 1977; and references therein) as showing that OB subgroups are formed in a step-wise process in which ionization and shock fronts produced by newly formed OB stars propagate into a molecular cloud, triggering the formation of the next generation of stars. Because of the complexity of the galactic center region, it is not possible to conclude with certainty that such a mechanism is operating here. However, we feel that the fact that a region of star formation near the galactic center should appear so much like those seen in spiral arms is extremely suggestive. It therefore seems possible that the mechanisms responsible for triggering star formation are substantially the same in the galactic center and in the spiral arms.

c) Helium Deficiency

Radio recombination line observations have revealed an apparent deficiency of helium in Sgr B2 and G0.5-0.0 (Churchwell, Mezger and Huchtmeier 1974). This is an important observational result because of the cosmological significance of the He/H ratio. Brown and Lockman (1975) have reported a detection of the H76α and He76α recombination lines from Sgr B2 and find a normal He/H ratio. They suggest that the low upper limit for the He/H ratio derived for Sgr B2 from observations of lower frequency recombination lines (Churchwell, Mezger, and Huchtmeier 1974) is a result of preferential enhancement of the lower frequency hydrogen lines by stimulated emission processes in the dense Sgr B2 molecular cloud. Brown and Lockman further suggest that this process may also account for the apparent deficiency of helium in G0.5-0.0.

The present data bear on this suggestion because they provide information on the physical conditions in the material surrounding the ionized regions in both Sgr B2 and G0.5-0.0 and show that the environments of these two sources differ dramatically from each other. In particular, Figure 1 shows that the Sgr B2 molecular cloud,which has a far infrared optical depth of unity and grain temperatures $\sim$ 30 K, is much denser and colder than is the material surrounding G0.5-0.0, where the far infrared optical depth is only $\sim$ 0.01 and the dust temperature is $\sim$ 70 K. Thus, if a stimulated emission process in the material outside of the H II region is responsible for the apparently low He/H ratio in both Sgr B2 and G0.5-0.0, this process must be able to operate under a rather wide range of physical conditions.

VI. CONCLUSIONS

1. The observed far infrared properties of H II regions near the galactic center, except perhaps for Sgr A, are in the range found for spiral arm H II region/molecular cloud complexes believed to be sites of recent and current star formation. Therefore these H II regions are very probably powered by O stars like those seen elsewhere in the Galaxy. It is not possible from the present data to identify the source of ionization in Sgr A.

2. The far infrared structure of Sgr B2 is consistent with current interpretations of this source as a region of extreme density in which star formation is proceeding.

3. The portion of the galactic plane between $\ell = 0^{\circ}.5$ and $0^{\circ}.7$ may be a site of sequential star formation such as is commonly seen in the spiral arms of the Galaxy.

TABLE 1

Source	Peak Flux* (Jy) 30 μ	50 μ	100 μ	Luminosity† ($L_\odot$) (25-130 μ)	Radio‡ (Jy)	T Color§ (°K)	T_g§ (°K)	$\tau_{50\mu}$§	Infrared Excess§
Sgr B2	6.9×10^2	6.5×10^3	3.0×10^4	2.7×10^6	15	39	32	>1	9
G0.6+0.0	$<1.0 \times 10^3$	2.8×10^3	4.9×10^3	6.3×10^5	3.8	56	43	0.1	9
G0.5+0.0(N)	1.3×10^3	1.7×10^3	1.1×10^3	3.6×10^5	2.7	100	65	0.01	7
G0.5+0.0(S)	1.3×10^3	2.1×10^3	1.4×10^3	4.1×10^5	3.0	100	65	0.01	7
G0.07+0.04	1.8×10^3	3.4×10^3	3.8×10^3	7.4×10^5	2.5	70	51	0.05	16
G0.01-0.12	$<2.0 \times 10^3$	1.8×10^3	1.4×10^3	3.6×10^5	1.5	90	60	0.01	13
Sgr A	6.5×10^3	1.2×10^4	7.6×10^3	2.3×10^6	28	100	65	0.05	4
G-0.01+0.02	1.5×10^3	3.4×10^3	2.6×10^3	6.3×10^5	3.4	90	60	0.02	10
Sgr C	7.1×10^2	2.1×10^3	1.8×10^3	3.8×10^5	5	80	55	0.02	7

*Measured into a 1' beam. For each object, the uncertainties are ±25% at each wavelength due principally to the calibration. This leads to systematic uncertainties of ±25% in the luminosities and ±15% in the temperatures.

†Peak luminosity into a 1' beam at an assumed distance of 10 kpc.

‡Measured into a 77" beam at 10.7 GHz (Downes 1974, Pauls et al. 1976) except for Sgr C, which is measured at 15.5 GHz into a 2'.2 beam (Kapitzky and Dent 1974).

§These quantities are defined in the Appendix. The tabulated quantities refer to the central 1'.

APPENDIX

Definition of Quantities Used in Analysis of the Far Infrared Data

(1) The far infrared luminosity is derived from integration of the observed energy distribution from 25 to 130 μm. Provided that the absorption optical depth of the dust in the vicinity of the H II region is on the order of, or greater than, unity at wavelengths between 0.1-1 μm, then essentially all of the energy radiated by the ionizing source will eventually be absorbed by dust and thermally re-radiated. Typically about two-thirds of this re-radiated energy falls within the 25-130 μm bands of the present experiment (Paper 1).

(2) The color temperature T_c is defined as the temperature of a Planck curve fit through the data. For the vast majority of far infrared sources the color temperature is greater than the brightness temperature, indicating that the emission is optically thin. Contributions to the observed radiation therefore generally come from all dust grains along the line of sight. An estimate of the physical grain temperature T_g is then commonly obtained (e.g., Harvey, Campbell, and Hoffmann 1976; Paper 1) by assuming that all grains along a single line of sight have the same temperature. Then, for grey grains, T_g equals T_c. For non-grey grains, T_g is obtained from fitting the data by a Planck function multiplied by a wavelength dependent grain absorption efficiency $Q(\lambda)$. All estimates of T_g in the paper are based on the assumed form $Q(\lambda) \propto \lambda^{-1}$ (Paper 1).

(3) An estimate of the optical depth of emission $\tau(\lambda)$ follows from the estimate of mean grain temperature T_g given in (2). For the optically thin case $\tau(\lambda)$ is approximately the ratio of the flux observed at a given wavelength λ to that expected from a blackbody of temperature T_g. By making assumptions about the properties of the grains this optical depth of emission can be converted to a mass column density of radiating dust (Paper 1).

(4) The infrared excess is a parameter which is a function of the relative far infrared luminosity and radio continuum brightness of an H II region. Its precise mathematical form is based on the historical idea that all the far infrared luminosity of an H II region might result primarily from heating of grains within the ionized gas by resonantly trapped Lyman α photons. The definition is (e.g., Jennings 1975).

$$\text{Infrared Excess} = \left(\frac{\text{Infrared Luminosity}}{\text{Lyman } \alpha \text{ Luminosity}} \right) - 1 \qquad \text{A.1}$$

where the Lyman α luminosity is the rate of recombinations in the H II region, determined from radio continuum observations, multiplied by the energy of a Lyman α photon.

Despite the failure of the idea motivating its definition, the infrared excess is still a useful parameter in the description of H II regions. Observationally, values for the infrared excess in spiral arm H II regions usually lie in the range 3 to 20 (Furniss, Jennings, and Moorwood 1974). Values in the range 3 to 5 follow naturally from the fact that only about one third of the energy of an O star is emitted as photons capable of

ionizing hydrogen, yet the dust in and just outside the region actually absorbs essentially all the stellar energy. Values larger than 5 can result if primary ionizing photons are absorbed by dust within the H II region; this would indicate a high density of dust within the ionized region. Alternatively, a large value of the infrared excess may indicate the presence of non-ionizing sources of luminosity; detailed studies of nearby H II regions indicate that these exist. These luminosity sources may be pre-main sequence objects (Werner, Becklin, and Neugebauer 1977). In either of these cases, a large value of the infrared excess is indicative of very recent star formation. An H II region excited by a late O or early B star would have a high infrared excess, but it would also have a far infrared luminosity much lower than the regions discussed here.

Because of the difficulty in estimating the size of the H II regions which are seen against the galactic plane, which is bright at both infrared and radio wavelengths, we assume that the H II regions are the same size at infrared and radio wavelengths, and use the definition (Jennings 1975):

$$\text{Infrared Excess} = 12.2 \times 10^{10} \left(\frac{\text{Infrared Flux (W m}^{-2})}{\text{Radio Flux (Jy)}} \right) - 1 \qquad \text{A.2}$$

Here the infrared and radio flux must, of course, be measured with the same size beam. The measurements of the radio fluxes referred to in this paper are mainly made with a 77" beam; we assume that the correction factor to the size of the infrared beam, 1 arcminute, is (60/77). Also, a factor of 1.5 has been included in the coefficient in A.2 to account for luminosity outside the band of the infrared experiment.

REFERENCES

Alvarez, J. A., Furniss, I., Jennings, R. E., King, K. J., and Moorwood, A. F. M. 1974, in H II Regions and the Galactic Centre, Proceedings of the Eighth ESLAB Symposium, ed. by A.F.M. Moorwood (Neuilly-sur-Seine: ESRO), p. 69.

Becklin, E. E., Matthews, K., Neugebauer, G., and Wynn-Williams, C. G. 1977, Astr. and Ap., 55, 19.

Brown, R. L. and Broderick, J. J. 1973, Ap. J., 181, 125.

Brown, R. L. and Lockman, F. J. 1975, Ap. J. (Letters), 200, L155.

Cameron, R. M., Bader, M., and Mobley, R. E. 1971, Appl. Opt., 10, 2001.

Churchwell, E., Mezger, P. G., and Huchtmeier, W. 1974, Astr. and Ap., 32, 283.

Downes, D. 1974, in H II Regions and the Galactic Centre," Proceedings of the Eighth ESLAB Symposium, ed. by A.F.M. Moorwood (Neuilly-sur-Seine: ESRO), p. 247.

Elmegreen, B. G. and Lada, C. J. 1977, Ap. J., 214, 725.

Furniss, I., Jennings, R. E., and Moorwood, A.F.M. 1974, in H II Regions and the Galactic Centre," Proceedings of the Eighth ESLAB Symposium, ed. by A.F.M. Moorwood (Neuilly-sur-Seine: ESRO), p. 61.

Gatley, I., Becklin, E. E., Werner, M. W., and Wynn-Williams, C. G. 1977, Ap. J., in press (Paper I).

Genzel, R., Downes, D., and Bieging, J. 1976, M.N.R.A.S., 177, 101P.

Harper, D. A. 1974, Ap. J., 192, 557.

Harvey, P. M., Campbell, M. F., and Hoffmann, W. F. 1976, Ap. J. (Letters), 205, L69.

Harvey, P. M., Campbell, M. F., and Hoffmann, W. F. 1977, Ap. J., in press.

Harvey, P. M., Hoffmann, W. F., and Campbell, M. F. 1975, Ap. J. (Letters), 196, L31.

Hoffmann, W. F., Frederick, C. L., and Emery, R. J. 1971, Ap. J. (Letters), 164, L23.

Ingersoll, A. P., Münch, G., Neugebauer, G., and Orton, G. S. 1976, in Jupiter, ed. T. Gehrels, University of Arizona Press, p. 197.

Israel, F. P. 1976, Ph.D. Thesis, University of Groningen.

Jennings, R. E. 1975, in H II Regions and Related Topics, Lecture Notes in Physics, Vol. 42, ed. T. L. Wilson and D. Downes (Springer-Verlag).

Kapitzky, J. E. and Dent, W. A. 1974, Ap. J., 188, 27.

Low, F. J. and Aumann, H. H. 1970, Ap. J. (Letters), 162, L79.

Martin, A. H. M. and Downes, D. 1972, Ap. Lett., 11, 219.

Mezger, P. G., Churchwell, E., and Pauls, T. 1974, in Stars and the Milky Way System, ed. L. N. Mauridis (Springer-Verlag).

Mezger, P. G. and Smith, L. F. 1977, Astr. and Ap., in press.

Oort, J. H. 1977, Ann. Rev. Astr. and Ap., 15, in press.

Pauls, T., Downes, D., Mezger, P. G., and Churchwell, E. 1976, Astr. and Ap., 46, 407.

Rieke, G. H., Harper, D. A., Low, F. J., and Armstrong, K. R. 1973, Ap. J. (Letters), 183, L67.

Righini, G., Simon, M., Joyce, R. R., and Gezari, D. Y. 1975, Ap. J. (Letters), 195, L77.

Scoville, N. Z., Solomon, P. M., and Penzias, A. A. 1975, Ap. J., 201, 352.

Thronson, H. A. 1977, Ph.D. Thesis, University of Chicago.

Werner, M. W., Becklin, E. E., and Neugebauer, G. 1977 Science, in press.

Werner, M. W., Gatley, I., Harper, D. A., Becklin, E. E., Loewenstein, R. F., Telesco, C. M., and Thronson, H. A. 1976, Ap. J., 204, 420.

Westbrook, W. E., Werner, M. W., Elias, J. H., Gezari, D. Y., Hauser, M. G., Lo, K. Y., and Neugebauer, G. 1976, Ap. J., 209, 94.

FIGURE CAPTIONS

Fig. 1 (a) - Upper Left. Map of the galactic plane between G0.5-0.0 and Sgr B2 at 50 μm. The contour levels are equivalent to 6, 12, 18, 24, 36, 48 and 60 times 100 Jy into a 1' beam (1 Jy = 10^{-26} W m^{-2} Hz^{-1}). The dashed contours through G0.5+0.0 have been interpolated through a location at which no scan was taken. The region approximately parallel to the galactic equator enclosed by the light dashed lines is the area mapped.

Fig. 1 (b) - Upper Right. Map of the G0.5-0.0/Sgr B2 region at 100 μm. The contour levels are equivalent to 1.5, 3, 6, 12, 18, 24 and 30 times 10^3 Jy into a 1' beam.

Fig. 1 (c) - Lower Left. A comparison of far infrared color temperature and optical depth of radiating dust with molecular column density. The light solid contours are the 50 μm surface brightness map of Fig. 1 (a). The large and small superposed numbers give the color temperature and optical depth of 50 μ emission respectively, derived as discussed in the Appendix. The dashed contours show the distribution of $\int N\ (^{13}CO)dV$, the total ^{13}CO column density given by Scoville, Solomon and Penzias (1975). The contour levels are 2, 4, 6 and 8 times 5.7×10^{16} cm^{-2}.

Fig. 1 (d) - Lower Right. A map of the 10.7 GHz radio continuum emission from the G0.5-0.0/Sgr B2 region (Downes 1974). The contour levels are 4, 8, 16, 24, 32, 48, 64 and 80 times 0.188 K T_a.

Fig. 2 - The 30 μ to 1 mm energy distribution of the central 1' of Sgr B2, and the far infrared energy distributions of the central 1' of G0.6-0.0 and of G0.5-0.0 (N). The 200 μ, 350 μ and 1 mm data are from Harvey, Campbell and Hoffmann (1977); Rieke et al.(1973); and Westbrook et al. (1976).

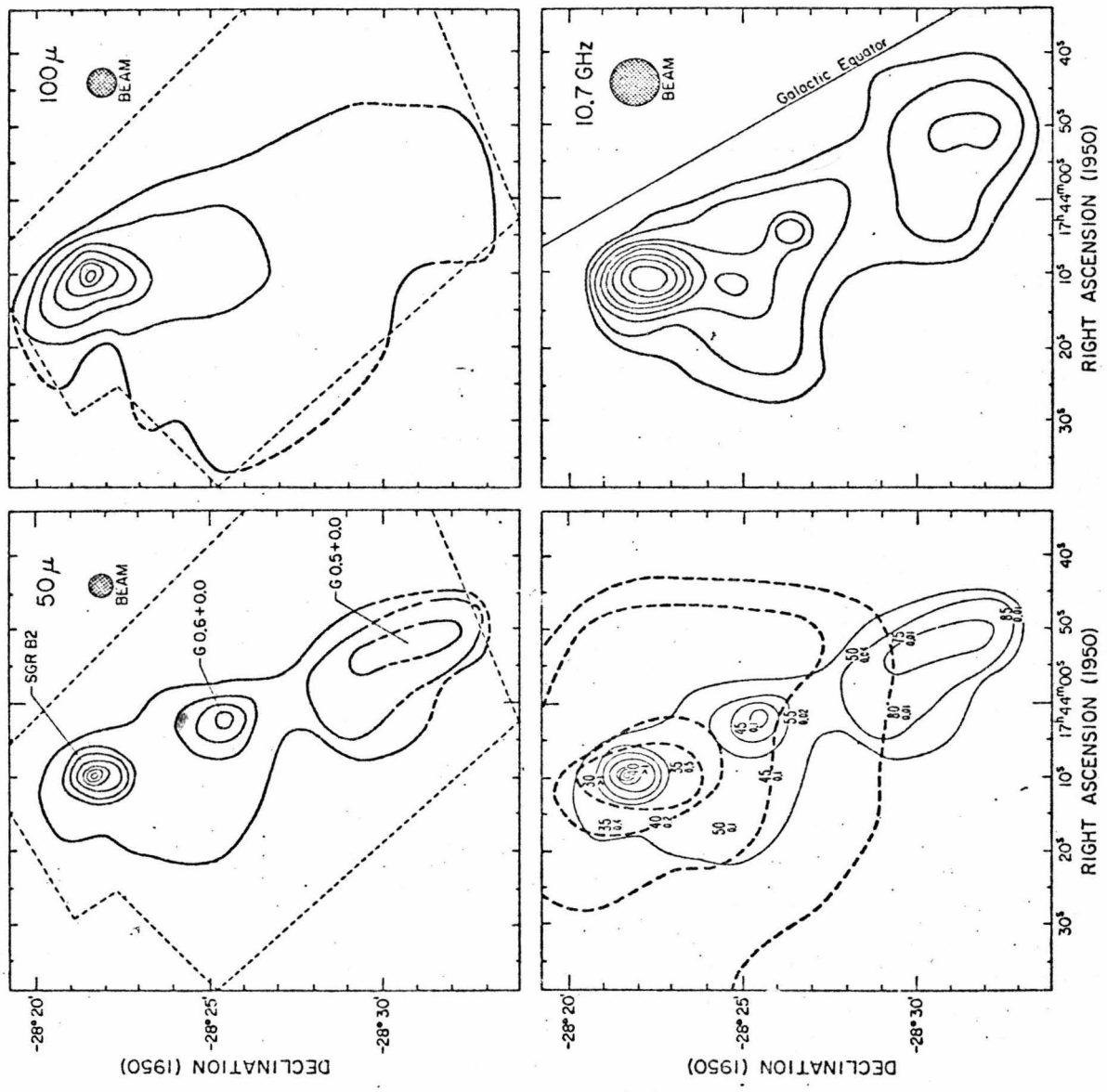
100 μ
BEAM
50 μ
BEAM
SGR B2
G 0.6+0.0
G 0.5+0.0
10.7 GHz
BEAM
Galactic Equator
-28° 20'
-28° 25'
-28° 30'
DECLINATION (1950)
30s
20s
10s
17h44m00s
50s
40s
RIGHT ASCENSION (1950)

Figure 1

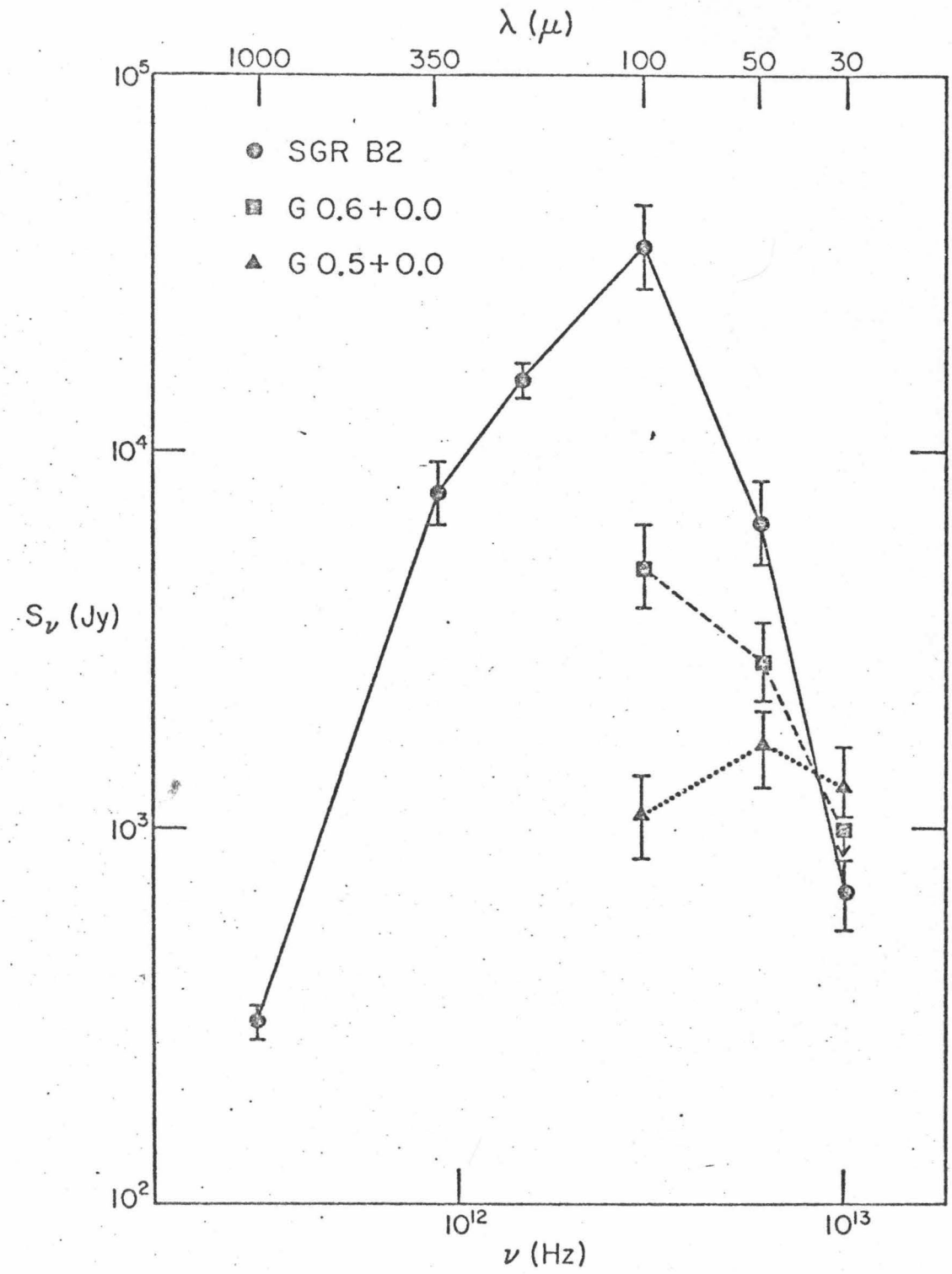
λ (μ)
1000
350
100
50
30
10^5
10^4
10^3
10^2
SGR B2
G 0.6+0.0
G 0.5+0.0
S_ν (Jy)
10^12
10^13
ν (Hz)

Figure 2